



# **Regional Stratigraphic Correlation and 3D Geological Modelling of West-Central Alberta**

**AER/AGS Open File Report 2019-04**

# **Regional Stratigraphic Correlation and 3D Geological Modelling of West-Central Alberta**

H.J. Corlett, T.L. Playter, M. Babakhani, B. Hathway, J.T. Peterson and  
K.E. MacCormack

Alberta Energy Regulator  
Alberta Geological Survey

June 2019

©Her Majesty the Queen in Right of Alberta, 2019  
ISBN 978-1-4601-3982-0

The Alberta Energy Regulator / Alberta Geological Survey (AER/AGS), its employees and contractors make no warranty, guarantee or representation, express or implied, or assume any legal liability regarding the correctness, accuracy, completeness or reliability of this publication. Any references to proprietary software and/or any use of proprietary data formats do not constitute endorsement by AER/AGS of any manufacturer's product.

If you use information from this publication in other publications or presentations, please acknowledge the AER/AGS. We recommend the following reference format:

Corlett, H.J., Playter, T.L., Babakhani, M., Hathway, B., Peterson, J.T. and MacCormack, K.E. (2019):  
Regional stratigraphic correlation and 3D geological modelling of west-central Alberta; Alberta  
Energy Regulator / Alberta Geological Survey, AER/AGS Open File Report 2019-04, 53 p.

Publications in this series have undergone only limited review and are released essentially as submitted by the author.

**Published June 2019 by:**

Alberta Energy Regulator  
Alberta Geological Survey  
4th Floor, Twin Atria Building  
4999 – 98th Avenue  
Edmonton, AB T6B 2X3  
Canada

Tel: 780.638.4491  
Fax: 780.422.1459  
E-mail: [AGS-Info@aer.ca](mailto:AGS-Info@aer.ca)  
Website: [www.ags.aer.ca](http://www.ags.aer.ca)

# Contents

Acknowledgements.....	viii
Abstract.....	ix
1 Introduction.....	1
2 Geological Background.....	1
2.1 Paleozoic.....	1
2.2 Mesozoic to Cenozoic.....	5
3 Methods.....	5
3.1 Stratigraphic Correlation.....	5
3.2 Modelling.....	6
3.2.1 2.5D Surface Modelling.....	6
3.2.2 Eroded Formations.....	7
3.2.3 Unconformities: Sub-Permian, Sub-Triassic, Sub-Jurassic, and Sub-Cretaceous.....	7
3.3 Building the 3D Model.....	8
3.3.1 Reefs and Onlapping Surfaces.....	8
3.3.2 Modelling Wedge-Shaped Formations (Cardium and Dunvegan Formations).....	10
3.3.3 Unconformities.....	10
4 Results: Formation Extents, Pick Criteria, and Reference Wells.....	12
4.1 Precambrian Basement.....	12
4.2 Watt Mountain Formation.....	12
4.2.1 Stratigraphic Interval and Extent.....	13
4.2.2 Pick Criteria and Reference Wells.....	13
4.3 Swan Hills Formation / Slave Point Formation.....	13
4.3.1 Stratigraphic Interval and Extent.....	13
4.3.2 Pick Criteria and Reference Wells.....	13
4.4 Waterways Formation.....	16
4.4.1 Stratigraphic Interval and Extent.....	16
4.4.2 Pick Criteria and Reference Wells.....	16
4.5 Majeau Lake Formation.....	16
4.5.1 Stratigraphic Interval and Extent.....	16
4.5.2 Pick Criteria and Reference Wells.....	16
4.6 Leduc Formation.....	17
4.6.1 Stratigraphic Interval and Extent.....	17
4.6.2 Pick Criteria and Reference Wells.....	17
4.7 Duvernay Formation.....	17
4.7.1 Stratigraphic Interval and Extent.....	17
4.7.2 Pick Criteria and Reference Wells.....	18
4.8 Ireton Formation and the Z-Marker Horizon.....	18
4.8.1 Stratigraphic Interval and Extent.....	18
4.8.2 Pick Criteria and Reference Wells.....	18
4.9 Nisku Formation.....	18
4.9.1 Stratigraphic Interval and Extent.....	19
4.9.2 Pick Criteria and Reference Wells.....	19
4.10 Calmar Formation.....	19
4.10.1 Stratigraphic Interval and Extent.....	19
4.10.2 Pick Criteria and Reference Wells.....	19
4.11 Graminia Formation.....	20
4.11.1 Stratigraphic Interval and Extent.....	20
4.11.2 Pick Criteria and Reference Wells.....	20
4.12 Wabamun Group.....	20

4.12.1	Stratigraphic Interval and Extent .....	20
4.12.2	Pick Criteria and Reference Wells .....	20
4.13	Exshaw Formation .....	21
4.13.1	Stratigraphic Interval and Extent .....	21
4.13.2	Pick Criteria and Reference Wells .....	21
4.14	Banff Formation .....	21
4.14.1	Stratigraphic Interval and Extent .....	21
4.14.2	Pick Criteria and Reference Wells .....	21
4.15	Pekisko Formation .....	22
4.15.1	Stratigraphic Interval and Extent .....	22
4.15.2	Reference Logs and Picking Criteria .....	22
4.16	Shunda Formation .....	22
4.16.1	Stratigraphic Interval and Extent .....	22
4.16.2	Reference Logs and Picking Criteria .....	22
4.17	Debolt Formation .....	25
4.17.1	Stratigraphic Interval and Extent .....	25
4.17.2	Reference Logs and Picking Criteria .....	25
4.18	Stoddart Group .....	25
4.18.1	Stratigraphic Interval and Extent .....	25
4.18.2	Reference Logs and Picking Criteria .....	27
4.19	Belloy Formation .....	27
4.19.1	Stratigraphic Interval and Extent .....	27
4.19.2	Reference Logs and Picking Criteria .....	27
4.20	Montney Formation .....	28
4.20.1	Stratigraphic Interval and Extent .....	28
4.20.2	Reference Logs and Picking Criteria .....	28
4.21	Schooler Creek Group / Doig Formation Interval .....	28
4.21.1	Stratigraphic Interval and Extent .....	28
4.21.2	Reference Logs and Picking Criteria .....	28
4.22	Nordeg Member .....	29
4.22.1	Stratigraphic Interval and Extent .....	29
4.22.2	Reference Logs and Picking Criteria .....	29
4.23	Fernie Formation .....	29
4.23.1	Stratigraphic Interval and Extent .....	29
4.23.2	Reference Logs and Picking Criteria .....	29
4.24	Nikanassin Formation .....	30
4.24.1	Stratigraphic Interval and Extent .....	30
4.24.2	Reference Logs and Picking Criteria .....	30
4.25	Cadomin Formation .....	30
4.25.1	Stratigraphic Interval and Extent .....	30
4.25.2	Reference Logs and Picking Criteria .....	30
4.26	Gething Formation / Ostracod Beds / Ellerslie Member Interval .....	30
4.26.1	Stratigraphic Interval and Extent .....	31
4.26.2	Reference Logs and Picking Criteria .....	31
4.27	Bluesky Formation .....	31
4.27.1	Stratigraphic Interval and Extent .....	31
4.27.2	Reference Logs and Picking Criteria .....	31
4.28	Spirit River Formation / Upper Mannville Group Interval .....	31
4.28.1	Stratigraphic Interval and Extent .....	32
4.28.2	Reference Logs and Picking Criteria .....	32
4.29	Harmon Member / Joli Fou Formation Interval .....	32

4.29.1	Stratigraphic Interval and Extent .....	32
4.29.2	Reference Logs and Picking Criteria .....	32
4.30	Viking Formation / Peace River Formation (excluding Harmon Member) Interval.....	32
4.30.1	Stratigraphic Interval and Extent .....	32
4.30.2	Reference Logs and Picking Criteria .....	33
4.31	Base of Fish Scales Marker.....	33
4.31.1	Stratigraphic Interval and Extent .....	33
4.31.2	Reference Logs and Picking Criteria .....	33
4.32	Belle Fourche Formation / Upper Shaftesbury Formation / Lower Kaskapau Formation Interval .....	33
4.32.1	Stratigraphic Interval and Extent .....	33
4.32.2	Reference Logs and Picking Criteria .....	35
4.33	Dunvegan Formation .....	35
4.33.1	Stratigraphic Interval and Extent .....	35
4.33.2	Reference Logs and Picking Criteria .....	35
4.34	Second White Specks Formation .....	35
4.34.1	Stratigraphic Interval and Extent .....	35
4.34.2	Reference Logs and Picking Criteria .....	36
4.35	Cardium Formation.....	36
4.35.1	Stratigraphic Interval and Extent .....	36
4.35.2	Pick Criteria and Reference Wells.....	36
4.36	Muskiki Formation / Upper Kaskapau Formation Interval.....	36
4.36.1	Stratigraphic Interval and Extent .....	37
4.36.2	Pick Criteria and Reference Wells.....	37
4.37	Lower Puskwaskau Formation / Bad Heart Formation / Marshybank Formation Interval.....	37
4.37.1	Stratigraphic Interval and Extent .....	37
4.37.2	Pick Criteria and Reference Wells.....	37
4.38	Lea Park Formation / Upper Puskwaskau Formation Interval.....	37
4.38.1	Stratigraphic Interval and Extent .....	37
4.38.2	Pick Criteria and Reference Wells.....	37
4.39	Wapiti Formation.....	38
4.39.1	Stratigraphic Interval and Extent .....	38
4.39.2	Pick Criteria and Reference Wells.....	38
4.40	Battle Formation .....	38
4.41	Scollard Formation.....	38
4.41.1	Stratigraphic Interval and Extent .....	38
4.41.2	Pick Criteria and Reference Wells.....	38
4.42	Sub-Cretaceous Unconformity.....	40
5	Discussion: Uncertainties and Future Work .....	40
5.1	Paleozoic Intervals for Investigation.....	43
5.2	Mesozoic Intervals for Investigation.....	44
5.3	Modelling Complications.....	44
6	Summary .....	45
7	References.....	46

## Tables

Table 1.	Calculated uncertainty for each modelled surface, including the root mean square error (RMSE).....	41
----------	--	----

## Figures

Figure 1. a) Study area location of the 3D geological model in west-central Alberta. b) Complete modelled volume showing stratigraphic intervals from the Precambrian basement to the top of the Paskapoo Formation. The uppermost surface represents present-day bedrock topography. Vertical exaggeration is 50 times. c) Colour legend, zone codes, and zone names.....	2
Figure 2. a) Select portions of the stratigraphic column of the west-central and northwest plains areas, Alberta. b) Legend explaining the colours and symbols used in the stratigraphic column.....	4
Figure 3. Variogram model of the Gething Formation generated using ArcMap.....	7
Figure 4. A subsection of the lower portion of the geological model highlighting the Leduc Formation reefs, west-central Alberta. ....	9
Figure 5. Dunvegan Formation is wedged between the top of the lower Kaskapau Formation and the top of the underlying upper Shaftesbury Formation. ....	10
Figure 6. A subsection of the middle portion of the geological model highlighting the sub-Cretaceous unconformity surface (west-central Alberta). ....	11
Figure 7. Stratigraphic cross-section A–A' showing representative picks for the interval from the Watt Mountain Formation to the Banff Formation.....	14
Figure 8. Stratigraphic cross-section B–B' showing representative picks for the interval from the Watt Mountain Formation to the Banff Formation.....	15
Figure 9. Stratigraphic cross-section showing representative picks for the interval from the Pekisko Formation to the base of the Fish Scales Formation. ....	23
Figure 10. Stratigraphic cross-section showing representative picks for the interval from the Pekisko Formation to the base of the Fish Scales Formation (cross-section datum).....	24
Figure 11. Two-dimensional maps of the unconformities in the west-central Alberta model. The coloured area represents the extent of the area affected by each unconformity in the 3D model: a) sub-Permian; b) sub-Triassic; c) sub-Jurassic; and d) sub-Cretaceous.....	26
Figure 12. Stratigraphic cross-sections A–A' and B–B'. a) A–A' shows representative picks for the interval from the base of the Fish Scales Formation to the base of the Wapiti Formation. b) B–B' shows representative picks for the Cardium Formation and Bad Heart / Marshybank formations. ....	34
Figure 13. Stratigraphic cross-section C–C' showing lateral variability in the relative stratigraphic level of the basal Paskapoo Formation sandstone interval.....	39

## **Acknowledgements**

We would like to thank our colleagues at the Alberta Energy Regulator / Alberta Geological Survey for their help with software, interpretations, and helpful discussions during the preparation of this report. Specifically, we would like to say a special thanks to Tyler Hauck and Dinu Pana who were generous with their advice and guidance throughout the project, and Matt Grobe for his review and comments on an earlier version of this report.

## **Abstract**

A three-dimensional (3D) geological model of west-central Alberta was created in partial fulfillment of the Alberta Geological Survey's Geological Framework objective of mapping and modelling the subsurface geology of Alberta. Model data were generated by correlating and mapping geological surfaces representing formation, member, or group tops in the subsurface. Sources of information used to generate pick data included wireline logs, drill core, and previous work published in the area. This geological model adds to the current understanding by clarifying complex stratigraphic relationships and important geological features that are present in west-central Alberta. A total of 49 geological surfaces were mapped using an average well spacing of 2 wells per township. The datasets of formation tops were modelled as two-and-a-half-dimensional (2.5D) surfaces and geostatistically evaluated for outlier data. These high quality datasets and accompanying surfaces were imported into a 3D modelling program where they were compiled and integrated into a 3D model, characterizing the subsurface geology. This report supports the first version of the 3D geological model of west-central Alberta and documents all steps taken to complete the model.

# 1 Introduction

A three-dimensional (3D) model of west-central Alberta ([Figure 1](#)) was created to visualize complex stratigraphic relationships and paleotopography in the subsurface. This study is part of the ongoing effort by the Alberta Geological Survey (AGS), part of the Alberta Energy Regulator (AER), to construct a 3D geological framework of Alberta (Branscombe et al., 2018a, b). The model helps visualize geological features such as faults and unconformities that may have an impact on resource extraction. Additionally, as a part of the larger geological framework of Alberta (Branscombe et al., 2018a, b), this model allows for the proper allocation of digital data collected in west-central Alberta by the AGS and AER. The datasets used to create the 3D geological model are available online as a public resource (<https://ags.aer.ca/data-maps-models/models.htm>).

The study area is located in west-central Alberta, covering 43 141.58 km<sup>2</sup> (6.5% of Alberta). A total of 49 geological surfaces, including regional unconformities, between the top of bedrock surface and the Precambrian basement were mapped. A minimum of two wells per township were used for mapping, wherever possible. After the pick datasets were compiled and modelled using Esri's ArcMap, they were evaluated for outliers and surfaces were compiled and modelled in three dimensions in Schlumberger's Petrel modelling program at a grid cell resolution of 500 by 500 m.

This report presents the first version of the 3D geological model of west-central Alberta, introduces the processes used to create the dataset used in the model, and defines the process involved in creating the model. With the addition of new data, particularly in data poor areas, future versions of the model will represent improvements of the first version. Not all of the geological complexities are included in this version of the model and potential future work is outlined in [Section 5](#).

## 2 Geological Background

The 3D geological model of west-central Alberta contains 49 surfaces from the Precambrian basement to the top of bedrock surface, including four unconformities within Permian and Mesozoic strata. The stratigraphic interval encompassed within this model begins at the base with the top of the Precambrian basement and ends with the Paskapoo Formation ([Figure 2](#)).

### 2.1 Paleozoic

During the Cambrian Period, a long transgression resulted in the migration of the paleoshoreline from the present-day Main Ranges in the Rocky Mountains to present-day central Saskatchewan, by the end of the late Cambrian (Aitken, 1968). In the west, thick sequences of carbonate and fine-grained clastic rocks were deposited at this time; however, erosion during the Early Devonian removed much of the Cambrian and overlying Ordovician deposits in the study area (Slind et al., 1994). Open marine seas flooded Alberta in the Early to Middle Devonian and a large barrier-reef system developed in the north on a Precambrian high known as the Tathlina Arch, which resulted in restriction within the basin until the middle Givetian (Wendte, 1992). Transgression in the Middle Devonian gave way to clastic deposition south of the Peace River Arch (PRA), which lies south of the Tathlina Arch and was located in western Alberta, and eventual development of a platform and reef complex (Swan Hills Formation; Oldale and Munday, 1994). Three major reef building events took place during the Late Devonian through a series of transgressive and regressive cycles, eventually filling the basin by the late Frasnian, during deposition of the Winterburn Group (Wendte, 1992). Carbonate rocks and associated evaporites of the Wabamun Group were deposited when a large carbonate ramp complex developed during the Famennian (Halbertsma, 1994). Following deposition of the Wabamun Group, a transgression and anoxic bottom waters resulted in deposition of the laminated black shales of the Exshaw Formation, followed by progradation during the deposition of the lower Banff Formation (Stoakes and Creaney, 1984).

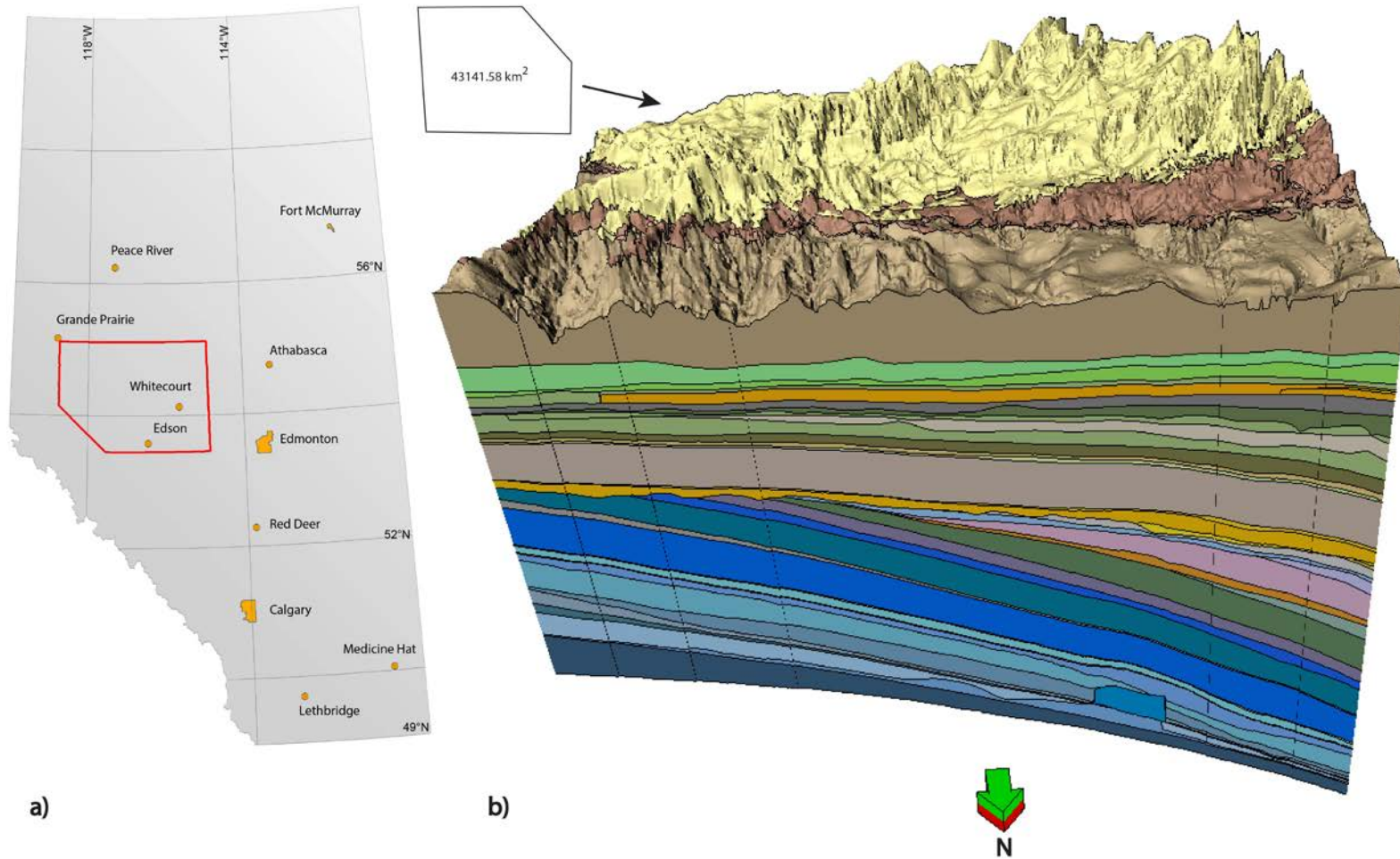


**Figure 1. a) Study area location of the 3D geological model in west-central Alberta. b) Complete modelled volume showing stratigraphic intervals from the Precambrian basement to the top of the Paskapoo Formation. The uppermost surface represents present-day bedrock topography. Vertical exaggeration is 50 times. c) [on next page] Colour legend, zone codes, and zone names used throughout this report.**

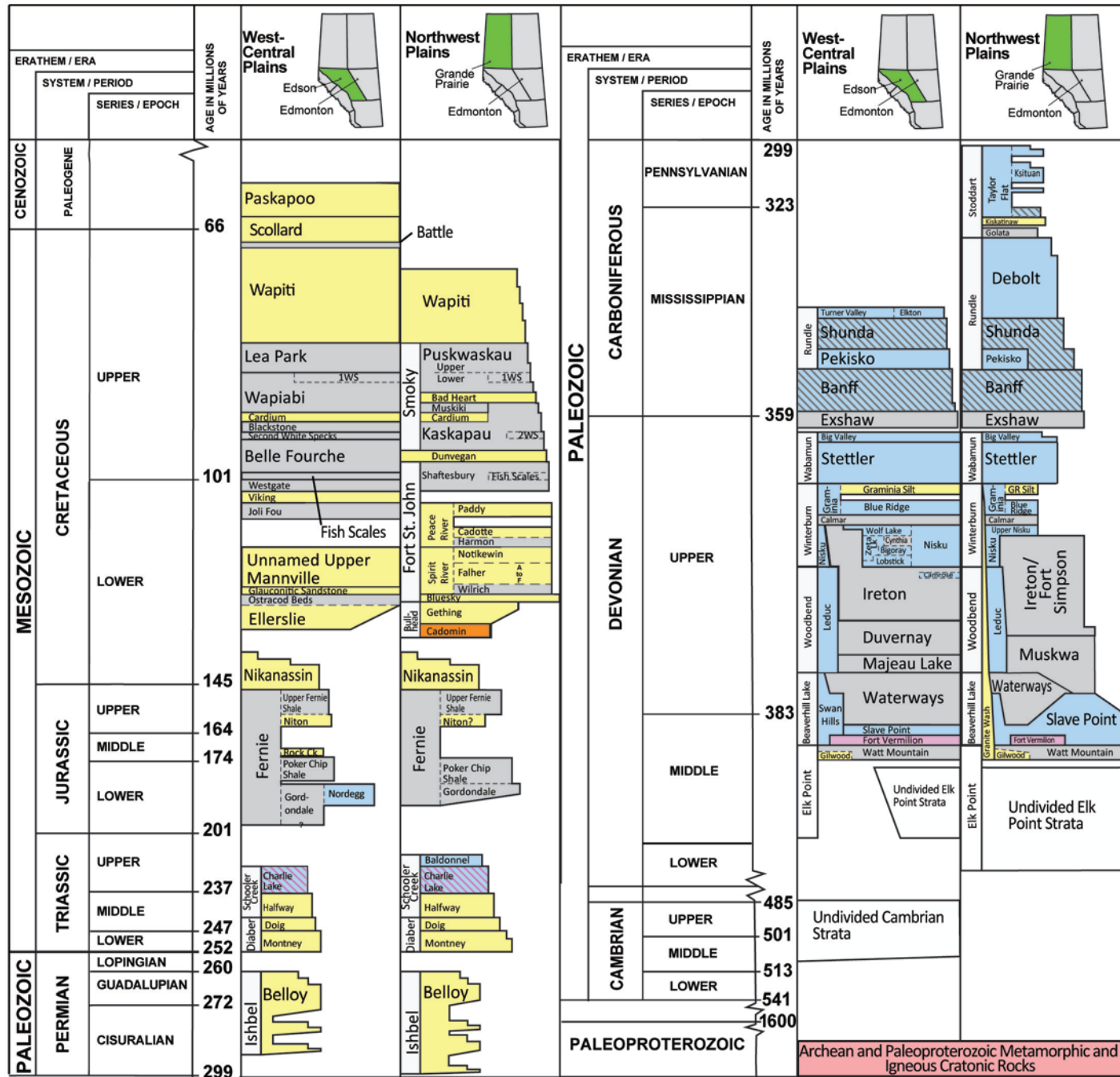
c) Legend for all Figures

Color, code, name:

	01 Pakapoo Formation		17 Westgate / lower Shaftesbury formations		33 Pekisko Formation
	02 Scollard Formation		18 Viking / Peace River formations (excluding Harmon Member)		34 Banff Formation
	03 Battle Formation		19 Joli Fou Formation / Harmon Member		35 Exshaw Formation
	04 Wapiti Formation		20 Spirit River Formation / upper Mannville Group		36 Wabamun Group
	05 Lea Park / upper Puskwaskau formations		21 Bluesky Formation		37 Graminia Silt Member
	06 lower Puskwaskau / Bad Heart formations		22 Gething Formation / Ostracod Beds / Ellerslie Member		38 Blue Ridge Member
	07 upper Kaskapau Formation		23 Cadomin Formation		39 Calmar Formation
	08 Muskiki Formation		24 Nikanassin Formation		40 Nisku Formation
	09 Cardium Zone Member		25 Fernie Formation (excluding Nordegg Member)		41 Ireton Formation (above Ireton Z marker)
	10 Cardium sandstone		26 Nordegg Member		42 Ireton Formation (below Ireton Z marker)
	11 Pembina River Member (excluding Cardium sandstone)		27 Schooler Creek Group / Doig Formation		43 Duvernay Formation
	12 Blackstone / middle Kaskapau formations		28 Montney Formation		44 Leduc Formation
	13 Second White Specks Formation		29 Belloy Formation		45 Majeau Lake Formation
	14 lower Kaskapau Formation		30 Stoddart Group		46 Waterways Formation
	15 Dunvegan Formation		31 Debolt Formation		47 Swan Hills / Slave Point formations
	16 Belle Fourche / upper Shaftesbury formations		32 Shunda Formation		48 Watt Mountain Formation to Precambrian interval

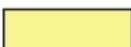
Figure 1 (continued). c) Colour legend, zone codes, and zone names used throughout this report.

a)



b)

### LITHOLOGY

-  Conglomerate and sandstone
-  Sandstone, siltstone, and quartzite, commonly interbedded with shale or mudstone
-  Shale and mudstone with subordinate siltstone
-  Limestone and dolostone
-  Limestone and dolostone interbedded with calcareous shale
-  Halite ± anhydrite, carbonate, and shale
-  Limestone and dolostone ± sandstone interbedded with anhydrite
-  Volcanic and volcanoclastic rock

### CONTACTS

-  Formation or group boundary
-  Member or unit boundary
-  Boundary uncertain
-  Boundary truncated by erosion
-  Lapout boundary or facies change

### ABBREVIATIONS

- 1WS First White Speckled Shale
- 2WS Second White Speckled Shale
- CK Creek
- GR Graminia
- LK Lake
- MTN Mountain

Figure 2. a) Select portions of the stratigraphic column of the west-central and northwest plains areas, Alberta. b) Legend explaining the colours and symbols used in the stratigraphic column. Adapted from the Alberta Table of Formations (Alberta Geological Survey, 2015).

Another period of sea-level rise initiated backstepping and aggradation of crinoid-rich carbonate ramps that comprise the Pekisko Formation carbonate rocks (Stoakes 1992a, b). The Shunda Formation was deposited during a final regressive stage in the late Tournaisian (Stoakes, 1992a, b). Transgression occurred during the deposition of the Pekisko and Debolt formations (Richards et al., 1994). Following this period of overall transgression, a regionally extensive subaerial exposure occurred along the southern portion of the Peace River Embayment (created through the collapse of the Peace River Arch; Richards et al., 1994). A subsequent period of tectonic subsidence during the late Carboniferous and Permian resulted in the deposition of the Stoddart Group and Belloy Formation, which infilled tectonically induced paleotopographic lows (Barclay et al., 1990). This marked a transition in tectonic regime from basement uplift, observed from the Precambrian to the lower Paleozoic, to subsidence (collapse of the Peace River Arch) and subsequent terrain accretion (Barclay et al., 1990).

## **2.2 Mesozoic to Cenozoic**

The mass extinction at the end of the Permian marked the beginning of a fundamental shift from Paleozoic carbonate-dominated sedimentary systems within the Western Canada Sedimentary Basin (WCSB) to the siliciclastic depositional systems of the Jurassic and Cretaceous (Davies, 1997). This transition period, during which the Triassic deposits (e.g., Montney Formation) of the WCSB were formed, was also a time of tectonic transition, which, by the Jurassic, included terrane accretion and the development of the foreland basin (Davies, 1997). A regionally extensive unconformity denotes the base of Jurassic deposition in the WCSB (Poulton et al., 1994). During the Early Jurassic, a phosphatic carbonate platform developed in the southeast part of the study area and was gradually overlain by foredeep deposits of shale and sandstone during the Late Jurassic, resulting in the Fernie Formation (Poulton et al., 1994). A major regional unconformity separates the Jurassic Fernie Formation and the Jurassic to lowermost Cretaceous Nikanassin Formation from the overlying Cretaceous Cadomin and Gething formations (Poulton et al., 1994). During the Early Cretaceous, the basin subsided and sea level rose, culminating with the early Albian transgression of the Boreal Sea (Hayes et al., 1994). Deposits of the Bullhead and Fort St. John groups are diverse, including initial fluvial deposits, and coal and alluvial fans of the Early Cretaceous and fully marine deposits of the late Albian (Reinson et al., 1994). Predominantly marine deposition continued for much of the Cretaceous, with marine and nonmarine interfingering occurring in the Late Cretaceous, recognized within deposits of the Smoky, Belly River, and Edmonton groups (Dawson et al., 1994). Uppermost Cretaceous and Cenozoic deposits, such as the Paskapoo Formation, were eroded after the Laramide Orogeny (Dawson et al., 1994). As much as 3 km of sediment was potentially removed (Dawson et al., 1994). Quaternary deposits of glacial, fluvial, organic, lacustrine, and eolian origin drape the unconformity (Fenton et al., 1994).

## **3 Methods**

### **3.1 Stratigraphic Correlation**

Correlations for the model commenced on May 31, 2014 and continued until May 31, 2015. Minor additional data were collected after this date on an as-needed basis for quality control during the creation of 2.5D surfaces. The picks used to build this model have not been previously published and include picks from the datasets of AGS geologists H. Corlett, B. Hathway, J. Peterson, T. Playter, T. Hauck, and from other AGS datasets. Over 2500 wells, including deviated wells, were examined and resulted in 61 247 picks used to geostatistically interpolate the form and geometry of the geological units in the study area. Wells along the zero- and subcrop-edges where the mapped geological unit was not present were included in the dataset to help constrain the lateral extent of the formation.

Stratigraphic tops were picked by geologists at the AGS using wireline logs. Drillcore at the AER Core Research Centre was examined and used to confirm stratigraphy in areas of complexity. In areas affected by erosion, stratigraphic-top data were separated into two groups: eroded formation tops and noneroded

formation tops, where formation tops located between the determined subcrop and zero edges were classified as eroded. Numerous references were used in the creation of this dataset to aid in regional correlation.

## **3.2 Modelling**

Stratigraphic data were modelled using a two-stage workflow: 1) stratigraphic tops were evaluated in ArcMap, creating 2.5D surfaces, and 2) the surfaces were imported into Petrel and integrated into a sealed 3D model. The resulting model highlights stratigraphic complexity in the area including eroded formations, regional unconformities, and reefs. These complexities required specific measures, such as isolating eroded data, merging surfaces, and the use of the convergent interpolator function in Petrel.

### **3.2.1 2.5D Surface Modelling**

The 2.5D surface grids for this model were built by geostatistically interpolating to unknown locations in each surface within the study area based on existing data. One of the most applicable estimation methods is kriging. Ordinary kriging is a linear geostatistical estimation method and is one of the most commonly used geostatistical tools since it is able to correspond to a nonstationary random function with an unknown mean (Deutsch and Journel, 1992). Lack of stationarity exists in the study area because of the first order trend. This type of kriging uses a variogram function to determine the optimal weights that should be assigned to nearby data to generate and estimate values of the surface at locations without data (Journel and Huijbregts, 1978).

All of the stratigraphic top datasets within this study area had a first order trend towards the mountains, reflecting the western dips in the foreland basin, which dominates western Alberta. It is important to make sure that all major trends are removed from the data prior to doing any geostatistical calculations. Most geostatistical methods are based on stationary analysis, which is not possible if there is a major trend in the dataset. A local polynomial algorithm was used to identify and model trends in each dataset. This trend surface was subtracted from the data prior to kriging.

Good quality data that has undergone major trend removal should produce an acceptable variogram model (Figure 3). The variogram must be evaluated and modelled for kriging estimation. Variogram parameters are defined on the distance between data points as lag size, the range of variogram coverage to have a proper lag number, and the direction of most and least continuity to define the short and long range continuity for variogram calculation. The short scale continuity is defined as the ‘nugget effect’.

Extreme outliers, verified to be geologically accurate by the geologist, are included by selecting a relatively small nugget effect. This ensures that the surface hits all the data points as closely as possible. There are several types of mathematical functions that approximate the shape of these variograms, such as Gaussian, exponential, and spherical models. The spherical model was most commonly used in kriging estimation for the west-central Alberta model.

The search neighbourhood radius for the chosen kriging method was determined by selecting the minimum and maximum number of surrounding data points that should be used to estimate the surface at locations with few or no data points. The search neighbourhood angles were defined based on the variogram model parameters.

Lastly, the uncertainty of the resulting surfaces was taken into account. By minimizing the uncertainty, the geomodeller is able to produce an unbiased surface, which honours the original data and is geologically realistic. High uncertainty typically occurs in areas that do not contain enough data to characterize the geology, and can be reduced by using larger search neighborhood radii, adding more nearby data points for estimation during kriging. High uncertainty may also occur in areas with outlier data representative of a geological structure or feature. This kind of uncertainty cannot be fixed because the anomalies that cause it represent real geological features of the surface. Reducing this type of uncertainty would require additional data points to better define the geological feature.

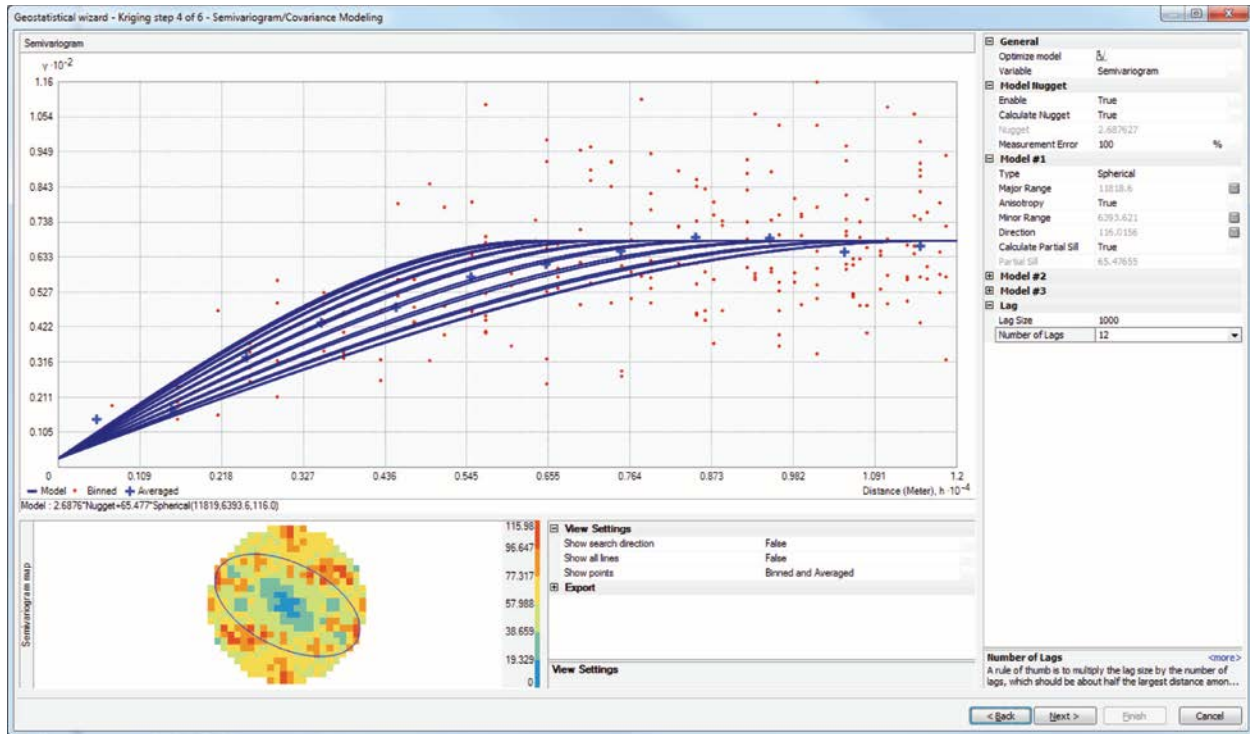


**Figure 3. Variogram model of the Gething Formation generated using ArcMap. The red dots in the graph are represented in the variogram map (bottom left) as coloured pixels. The average binned variogram values are shown as blue crosses in the graph. Blue lines represent the variogram model for different directions. The minor range is defined by the variogram model that first approaches the sill (flat line), and the last variogram to reach the sill defines the major range. The nugget effect is defined as the variogram value at the y-intercept (2.68 in this example).**

The reef-related 2.5D surfaces were built using the convergent interpolation algorithm in Petrel because of the increased complexity. All of the data points for these surfaces were geostatistically evaluated in ArcMap to identify potential outliers or erroneous data points, and once all the data had been verified, they were imported into Petrel as a point set and then modelled into 2.5D surfaces using the convergent interpolation algorithm.

### **3.2.2 Eroded Formations**

Several of the formations in this study are either partially or fully eroded. Unlike stratigraphically continuous surfaces, the tops of formations affected by regional-scale erosion were divided into two datasets (eroded and noneroded). This specification was necessary to ensure that only the noneroded points were used to model the geological surfaces. The points identified as eroded were retained to assist with modelling the unconformity surfaces (Section 3.2.3). The subcrop edge for each formation, member, or group of interest was used to verify this differentiation. The noneroded top data points were used to create a surface for the respective formation, member, or group of interest. This results in a surface that honours the data points up to the subcrop line. At the subcrop line, the formational surface intersects the overlying unconformity surface that is associated with the erosion of that particular formation and ensures that it is not present above the unconformity surface.

### **3.2.3 Unconformities: Sub-Permian, Sub-Triassic, Sub-Jurassic, and Sub-Cretaceous**

Within the study area, seven major unconformities are present: the Precambrian top surface, the sub-Devonian unconformity, the sub-Permian unconformity, the sub-Triassic unconformity, the sub-Jurassic

unconformity, the sub-Cretaceous unconformity and the bedrock top surface. Four of these major unconformity surfaces are included within the model and were constructed by combining the eroded stratigraphic tops from all formations that were truncated by the respective unconformity. Combining these picks allowed each unconformity to be modelled as an independent surface. The stratigraphically lowest major unconformity surface is the sub-Permian unconformity, which is made up of the eroded tops of the Stoddart Group and Debolt Formation, where overlain by Permian strata. The next major unconformity surface, stratigraphically younger than the sub-Permian unconformity, is the sub-Triassic unconformity, which is made up of the eroded tops of the Belloy, Debolt, and Shunda formations, where overlain by Triassic strata. The third unconformity surface is the sub-Jurassic unconformity surface that is composed of the eroded tops of the Charlie Lake and Doig (Upper Triassic), Montney, Debolt, Shunda, and Pekisko formations, where overlain by Jurassic strata. The uppermost unconformity surface is the sub-Cretaceous unconformity, which represents a significant period of erosion. In the study area the sub-Cretaceous unconformity surface is composed of the eroded tops of the Nikanassin and Fernie formations, Nordegg Member, and many of the formations mentioned above, where overlain by Cretaceous strata.

### **3.3 Building the 3D Model**

The 3D model was built in Petrel using the 2.5D surfaces created in ArcMap. Reef surfaces, onlapping surfaces, and unconformity surfaces required additional steps before they were incorporated into the 3D model. Each of these geological complexities and associated modelling techniques are explained fully in [Sections 3.3.1](#) and [3.3.2](#).

#### **3.3.1 Reefs and Onlapping Surfaces**

Several of the Paleozoic formations in the study area contain reef buildups. Two formations (the Swan Hills and Leduc formations) contain large buildups that required an alternative method to accurately model their top surfaces.

The Swan Hills Formation top surface was modelled in Petrel using the convergent interpolator and the Slave Point Formation surface was modelled in ArcMap using the kriging workflow described previously. An important step is to properly differentiate the platform and bank edges of the Swan Hills Formation reef complex from its stratigraphic basinal equivalent, the Slave Point Formation. The top surfaces of the Swan Hills and Slave Point formations were each cut based on their respective extent lines and then merged together to produce a single unified Swan Hills / Slave Point formations surface.

Modelling of the Leduc Formation reefs was more complex due to their extreme thickness (>300 m in some places) ([Figure 4](#)). The Leduc Formation reefs are surrounded, but not onlapped, by the Majeau Lake Formation. The Majeau Lake Formation onlaps or overlies the Beaverhill Lake Group, depending on the thickness of the Swan Hills Formation reefs. In the areas where the Swan Hills Formation reefs are particularly thick, the Majeau Lake Formation onlaps the reefs, and in areas where the Swan Hills /Slave Point formations interval is not as thick, the Majeau Lake Formation overlies the Waterways Formation of the Beaverhill Lake Group.

Some formations are discontinuous within the study area and show onlapping relationships, however the modelling process produces continuous surfaces, which then need to be cropped to the known formational extent to display these relationships accurately. This is true for the formations which onlap the Leduc reefs. For example, the Majeau Lake Formation is not present in the Wild River sub-basin. This absence required the top surface generated from the Majeau Lake Formation top dataset to be cropped. This cropped surface was then merged with the Waterways Formation top surface (which underlies the Majeau Lake Formation) to create a continuous, geologically accurate horizon. Outside of the Wild River sub-basin, where the Majeau Lake Formation is present, the Majeau Lake onlaps the Leduc reefs (where the Leduc reefs are present). To illustrate this, the Majeau Lake Formation top surface was merged with that of the Leduc Formation (which was also clipped to its known extent) in this area. Within the Wild River sub-basin, where the Majeau Lake Formation is absent, the Leduc Formation top surface was merged with

that of the Waterways Formation. Likewise, the Leduc Formation top surface was clipped to its known extent and merged with that of the Majeau Lake Formation. To represent the onlap of the Duvernay Formation, Z-marker horizon, and Ireton Formation onto the Leduc reefs, each surface was likewise clipped to its known extent and merged with the Leduc top surface.

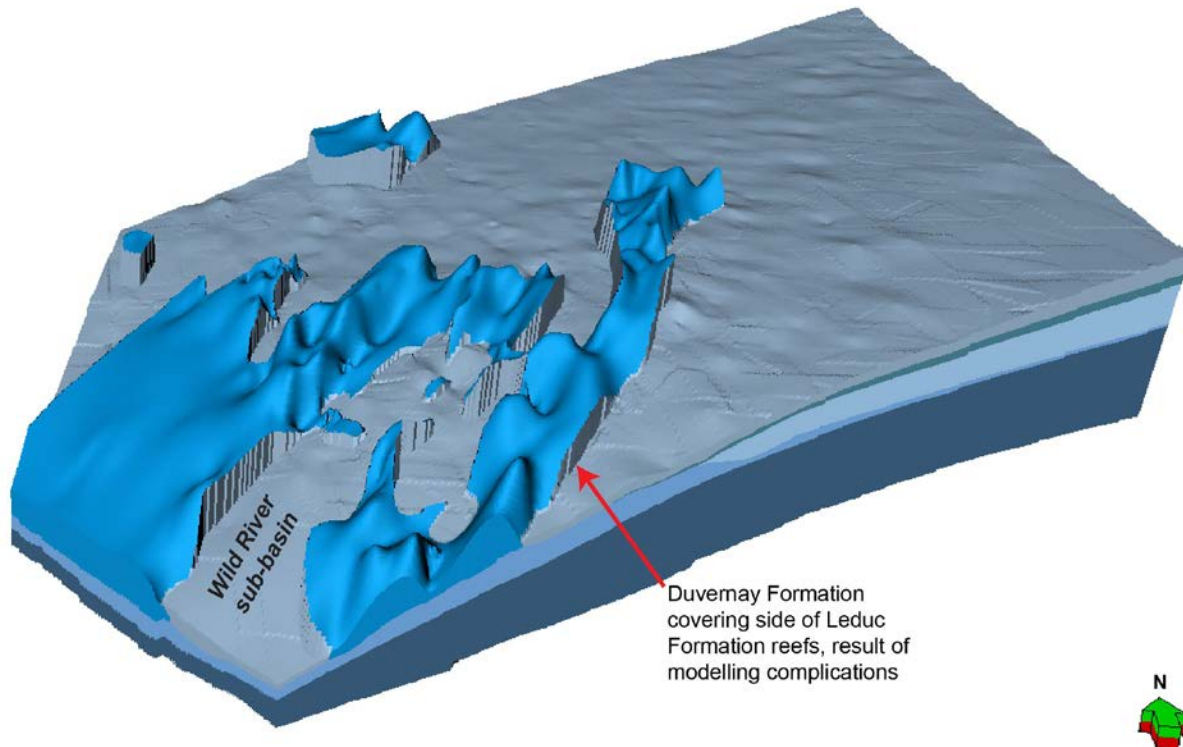


**Figure 4. A subsection of the lower portion of the geological model highlighting the Leduc Formation reefs, west-central Alberta. Additionally, a modelling error is noted in the figure. Vertical exaggeration is 50 times. Refer to Figure 1c for legend of stratigraphic unit names.**

Uncertainty analysis for these surfaces was performed by cross-validation of results obtained using a combination of MathWorks' MATLAB and ArcMap. The root-mean-square error (RMSE) values are used to represent the uncertainty of each surface because they provide a measure of the magnitude of the estimation error, which is defined as the standard deviation of the differences between the predicted value and observed value

$$RMSE = \sqrt{E((\hat{\theta} - \theta)^2)}$$

where  $\hat{\theta}$  is the predicted value,  $\theta$  the observed value, and  $E$  represents the averaging function.

The RMSE values were calculated using a MATLAB script that calculated the difference between the observed values (picks) and the values of the interpolated surface built by the convergent interpolator in Petrel in the same location. The uncertainty map of each surface was created based on the standard deviation of multiple realizations, which highlights areas with high variations in uncertainty values. Comparison of the uncertainty results from ArcMap surfaces and Petrel surfaces indicates that the Petrel surfaces provided more geologically accurate representations of the geology with lower uncertainty.

### 3.3.2 Modelling Wedge-Shaped Formations (*Cardium and Dunvegan Formations*)

The model area contains multiple zones with lithological pinch-outs, meaning that certain formations are encapsulated within another formation. Examples of this are the Cardium and Dunvegan formations. All surfaces within the model must extend across the entire model domain to avoid cell volumes not being allocated to a geological unit. Therefore, for wedge-shaped units that do not cover the entire domain, the underlying unit top was intentionally raised to be equal to the formation top overlying the wedge ([Figure 5](#)) just beyond the zero-edge (maximum extent) of the wedge-shaped formation. This prevented the wedge-shaped formation from being over extrapolated beyond its extent.

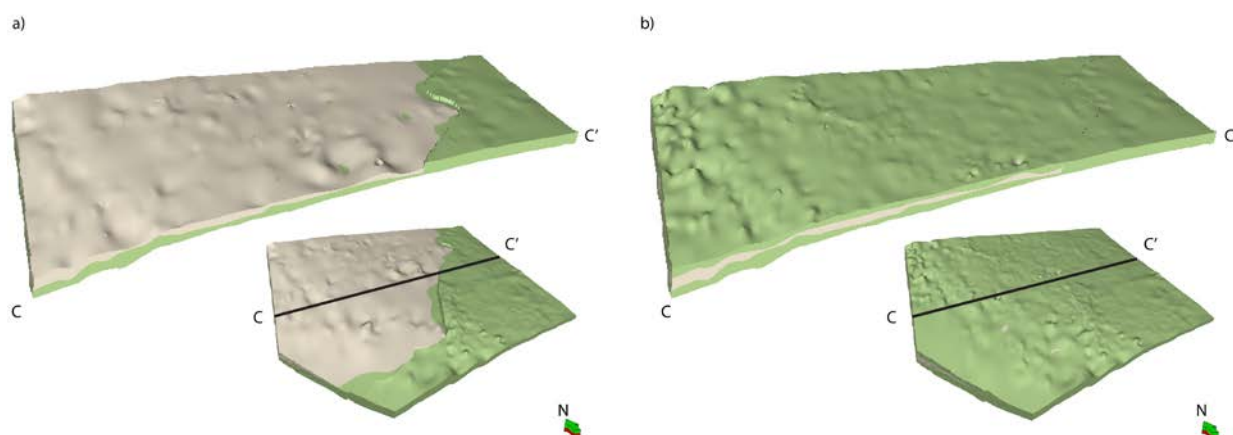


**Figure 5. Dunvegan Formation (shown in cream) is wedged between the top of the lower Kaskapau Formation and the top of the underlying upper Shaftesbury Formation (shown in green; west-central Alberta). Outside of Dunvegan Formation extent, the lower surface, was intentionally merged with the stratigraphically younger Belle Fourche Formation top surface (a), which allows the Dunvegan Formation to be modelled as a proper wedge (b). Refer to Figure 1c for legend of stratigraphic unit names.**

### 3.3.3 Unconformities

Unconformities mark intervals of nondeposition and/or erosion between successive strata. This model area contains four unconformity surfaces. A portion of each unconformity in the study area was subsequently eroded by a younger unconformity, except the sub-Cretaceous unconformity ([Figure 6](#)). To ensure the unconformity surfaces were properly rendered, they were merged in geological order from the oldest to youngest using their respective extent lines. This process is similar to that done to produce onlapping surfaces at the Leduc reefs. Each formation which subcrops at a given unconformity, is first clipped at its subcrop edge, which denotes the boundary where the unconformity surface intersects that formation. This separates the formation top surface into an eroded, subcropping portion and a non-eroded portion. By merging the subcrop portions of each formation top surface at the subcrop boundaries, a complete unconformity surface can be rendered.

The sub-Permian unconformity surface was merged with the portion of the sub-Triassic unconformity surface beyond the Belloy Formation zero edge, which was merged with the portion of the sub-Jurassic unconformity surface beyond the Montney Formation zero edge ([Figure 6](#)). The surface produced by merging these three unconformity surfaces was subsequently merged with the portion of the sub-Cretaceous unconformity surface beyond the Fernie Formation extent line. This produced a final merged continuous surface, comprised of portions of four individual discrete unconformity surfaces and extending across the entire study area. During model construction, the final merged continuous surface was used as a single sub-Permian unconformity surface to constrain the pre-Permian strata within the model volume. The same procedure was applied to create the sub-Triassic surface (a merger of the sub-

Triassic unconformity surface with the portions of the sub-Jurassic and sub-Cretaceous unconformity surfaces beyond the zero edges of the Montney Formation and Nordegg Member, respectively). The final stage of building the unconformity surfaces involved merging the sub-Jurassic unconformity surface with the portion of the sub-Cretaceous discrete surface beyond the Nordegg Member extent line, producing the regionally continuous surface that was used to constrain pre-Jurassic strata in the model.

By merging the individual unconformity surfaces, each resultant continuous unconformity surface was designated as ‘erosional’ in the process of making the 3D model in Petrel. By designating these unconformities surfaces as erosional, the underlying surfaces were modelled up to the unconformity surface and then truncated.

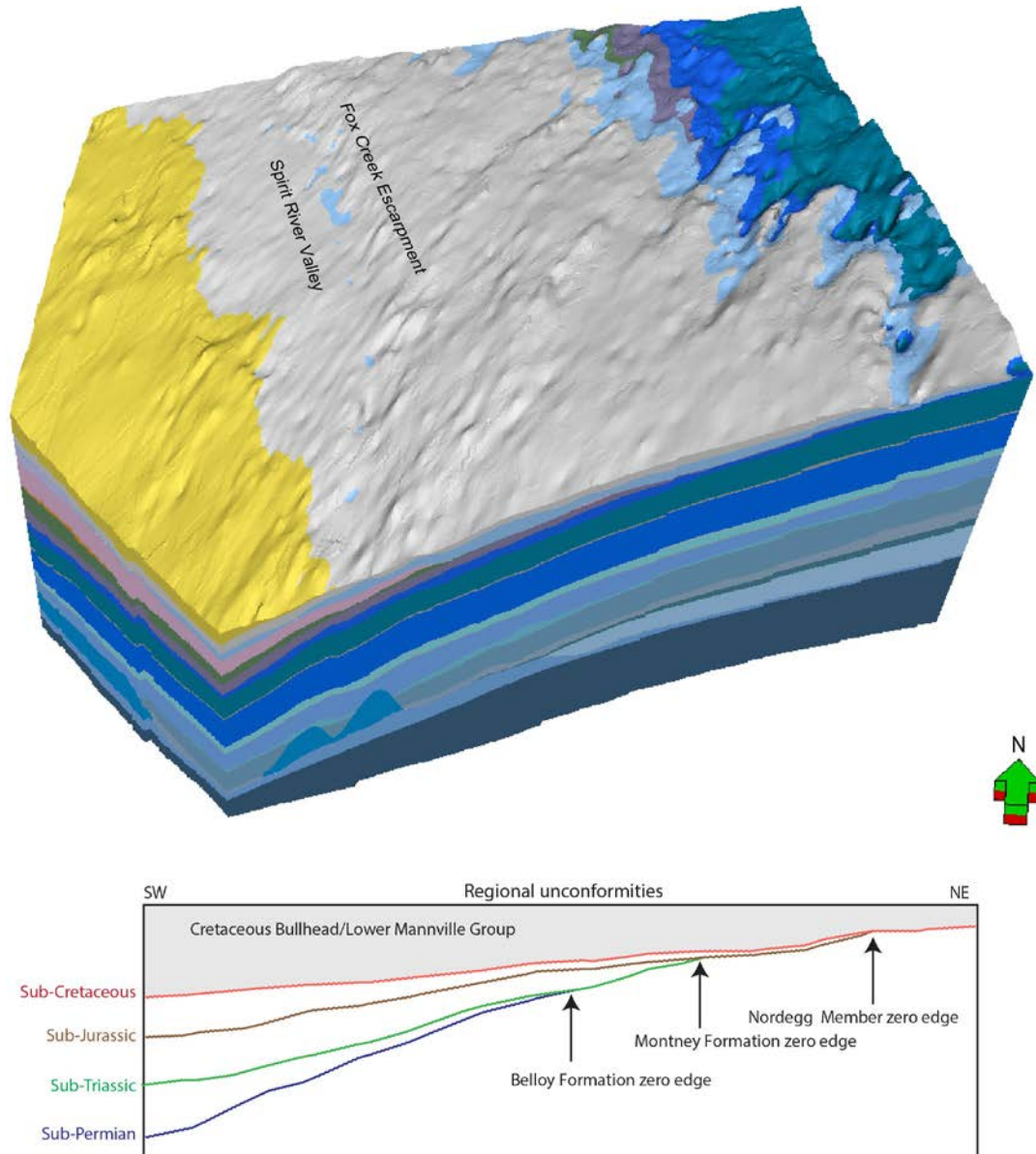


**Figure 6. A subsection of the middle portion of the geological model highlighting the sub-Cretaceous unconformity surface (west-central Alberta). Paleotopographic features such as the Fox Creek Escarpment and the Spirit River Valley are visible. A schematic cross-section is also included that depicts the relationship of the four major unconformity surfaces. Vertical exaggeration is 50 times. Refer to Figure 1c for legend of stratigraphic unit names.**

## 4 Results: Formation Extents, Pick Criteria, and Reference Wells

The surfaces correlated, mapped, and modelled in this model provide a geological framework for west-central Alberta encompassing strata between the Precambrian basement and the bedrock surface. The data used to create the modelled surfaces were correlated using wireline logs and stratigraphic interpretations were supported by peer-reviewed publications. This section contains a brief description of each stratigraphic interval, its distribution and extent, and the reference material used for picking the top of the unit or horizon.

Please note the following points of clarification on lateral stratigraphic or nomenclature boundaries present within the model:

- The Swan Hills Formation and Slave Point Formation were mapped together as one geological unit within the 3D geological model (referred to as the Swan Hills Formation / Slave Point Formation model zone). The top dataset for the Swan Hills and Slave Point formations includes the tops of reefs, platforms, and banks in the Beaverhill Lake Group ('Swan Hills Formation'), and of the off-platform basinal equivalent carbonate rocks ('Slave Point Formation').
- The boundary between the Peace River Formation and the Viking Formation occurs in west-central Alberta. At a regional scale, the Harmon Member of the Peace River Formation and the Joli Fou Formation form a mappable interval (referred to as the Joli Fou Formation / Harmon Member zone in the model). Likewise, the Paddy and Cadotte members of the Peace River Formation and the Viking Formation form a mappable interval (referred to as the Viking Formation / Peace River Formation (excluding the Harmon Member) zone in the model).
- The boundary between the upper Mannville Group strata and the Spirit River Formation of the Smoky Group also occurs within the study area; however, together they form a regionally mappable geological unit (referred to as the Spirit River Formation / upper Mannville Group model zone in the model).
- The study area includes the boundary between the Colorado Group and Fort St. John and Smoky groups, which occurs at the southeastern limit of the Dunvegan Formation. Because the model straddles numerous lithostratigraphic nomenclature boundaries, correlative unit tops are combined to form laterally continuous surfaces.

### 4.1 Precambrian Basement

The top of the Precambrian basement is marked by an unconformity. Crystalline rocks of the Canadian Shield are covered with Phanerozoic sediments. The top of Precambrian basement was modelled using picks from AGS geologists. The Precambrian basement is rarely accessed during oil and gas exploration, therefore well log data for this interval is sparse. To compensate for this, the Precambrian unconformity was modelled on the provincial scale, using all available data (5691 data points), and then cropped to the study area.

The stratigraphic interval between the top of the Precambrian and the top of the Watt Mountain Formation has not been broken down into individual stratigraphic intervals for this version of the model and includes strata of the Elk Point Group and Cambrian System.

### 4.2 Watt Mountain Formation

The top of the Watt Mountain Formation is considered to be equivalent to the top of the Devonian Elk Point Group (Wendte and Uyeno, 2005). Within proximity of the Peace River Arch (PRA), the Watt Mountain Formation contains the Gilwood Member, a coastal deltaic facies sourced from the PRA (Williams, 1997). The Watt Mountain Formation was deposited in a coastal plain to marginal-marine setting and comprises predominantly mudstone with intervals of interbedded sandstone and siltstone of varying mineral content (Kramers and Lerbekmo, 1967; Wendte and Uyeno, 2005).

### **4.2.1 Stratigraphic Interval and Extent**

The Watt Mountain Formation is present throughout the study area and thins away from the Peace River Arch (Rottenfusser and Oliver, 1977; Hauck, 2014). The Watt Mountain Formation overlies a regional unconformity that is present within the Elk Point Group, referred to as the sub-Watt Mountain unconformity (Meijer Drees, 1994).

### **4.2.2 Pick Criteria and Reference Wells**

The Watt Mountain Formation was picked in 677 wells in west-central Alberta. The subsea depths for the pick dataset range from -1240.9 to -3964.6 m. The high gamma-ray and low resistivity log signatures of the Watt Mountain Formation were used for correlation (Figures 6 and 7). These signatures are consistent throughout the study area. Information in Wendte and Uyeno (2005) along with cross-sections in Meijer Drees (1994) were used as a guideline for picking the top of the Watt Mountain Formation in the study area.

## **4.3 Swan Hills Formation / Slave Point Formation**

For the purposes of this study, the Swan Hills Formation and the Slave Point Formation tops were correlated as two separate surfaces and then merged within the 3D model (Figures 1, 7, and 8). The study area includes the Swan Hills Formation reef or bank complex that formed south of the fringing reefs of the Beaverhill Lake Group surrounding the Peace River Arch. The Swan Hills Formation reef complex developed over a long phase of transgression with several smaller transgressive-regressive cycles (Stoakes and Wendte, 1987; Wendte and Uyeno, 2005). Back-stepping reefs form the main Swan Hills Formation reef complex. Facies indicative of open-marine and basinal carbonate environments predominate in areas between the main reef complexes, and a burrow-nodular texture is commonly observed. These open-marine and basinal carbonate rocks have been mapped as the Slave Point Formation.

### **4.3.1 Stratigraphic Interval and Extent**

The Slave Point and Swan Hills formations overlie the Fort Vermilion Formation in the northeastern portion of the study area. Where the Fort Vermilion Formation is not present, the Slave Point and Swan Hills formations overlie the Watt Mountain Formation. The Fort Vermilion Formation is a thin unit (<5 m) that pinches out and has not been included as a separate unit in this version of the model. The combined top surface of the Slave Point Formation and the Swan Hills Formation extends throughout the study area. Both the Swan Hills Formation and the Slave Point Formation are overlapped by the Waterways Formation, which filled in the remaining accommodation space in the basin during Beaverhill Lake Group deposition through a series of transgressive and regressive cycles (Wendte and Uyeno, 2005).

A zero edge was created to denote the boundary of the Swan Hills Formation reef complex and the open-marine carbonate facies of the Slave Point Formation. This boundary was created using Figure 6 in Wendte and Uyeno (2005) as a guideline to distinguish between the edge of the carbonate reef or bank margin of the Swan Hills Formation and the open-water facies of the Slave Point Formation. Their regional study of the Beaverhill Lake Group included detailed examination of wireline logs, drillcore, and thin sections with a particular focus on differentiation of depositional facies.

### **4.3.2 Pick Criteria and Reference Wells**

The Swan Hills and Slave Point formations were picked in 818 wells. The subsea depths for the pick dataset range from -1230.2 to -3846.1 m. The regional studies of the Beaverhill Lake Group by Wendte and Uyeno (2005) and Hauck (2014) were used to guide correlation of both the Swan Hills Formation and the Slave Point Formation tops. Neutron porosity and bulk density logs were used to differentiate the Leduc Formation in areas where the Leduc Formation reefs developed directly on top of the Swan Hills Formation reefs.

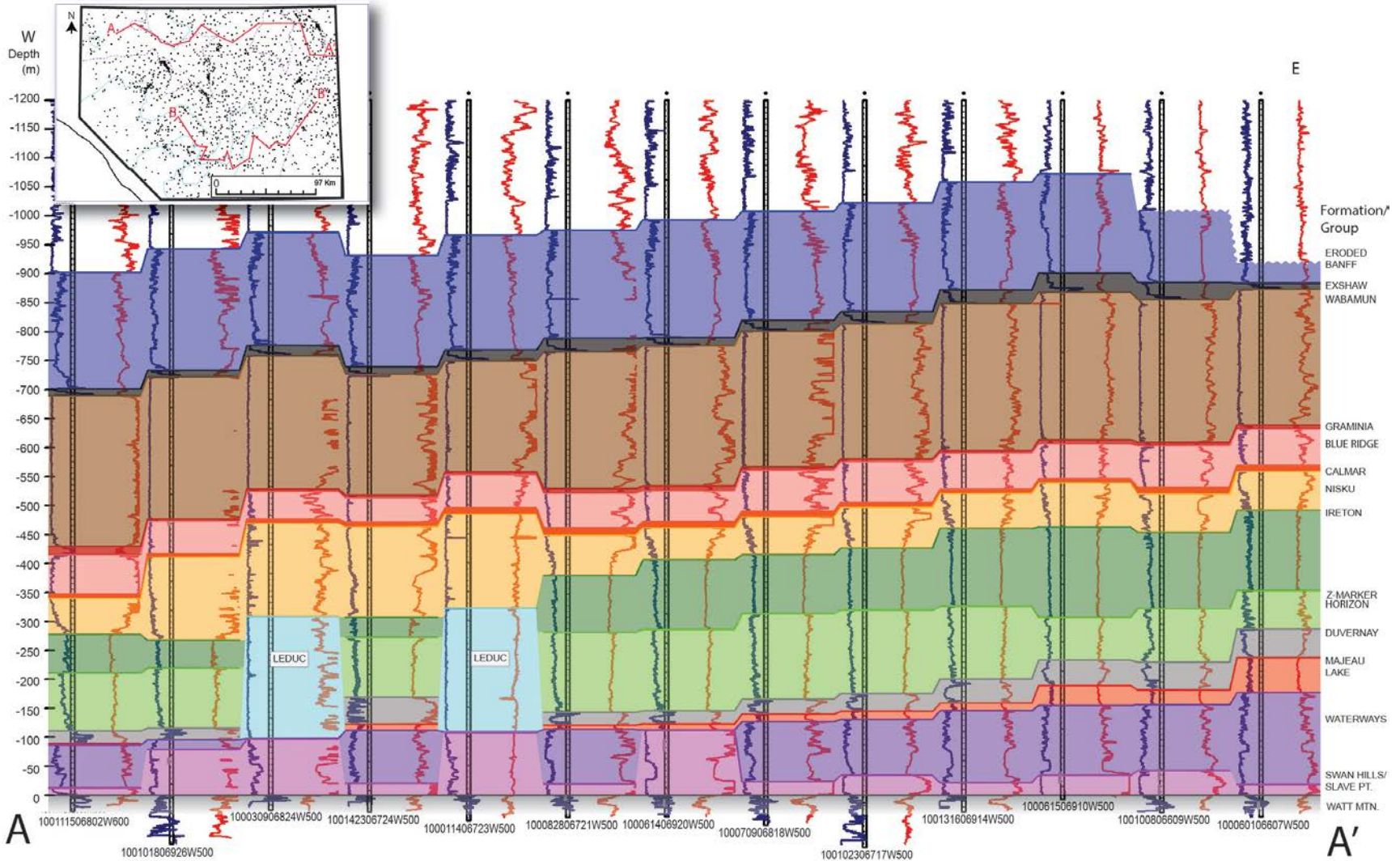


**Figure 7. Stratigraphic cross-section A–A' showing representative picks for the interval from the Watt Mountain Formation to the Banff Formation (Watt Mountain datum). Well-log traces include gamma ray (red) and resistivity (blue). Regional markers include the Z-marker horizon within the Ireton Formation and the base of the Exshaw Formation. The western portion of the cross-section highlights some of the complications surrounding contiguous, stacked reef successions, shown by the absence of the Z-marker horizon in some wells. These intervals contain the Leduc Formation reef buildups (light blue). Inset map shows location of cross-section, west-central Alberta.**

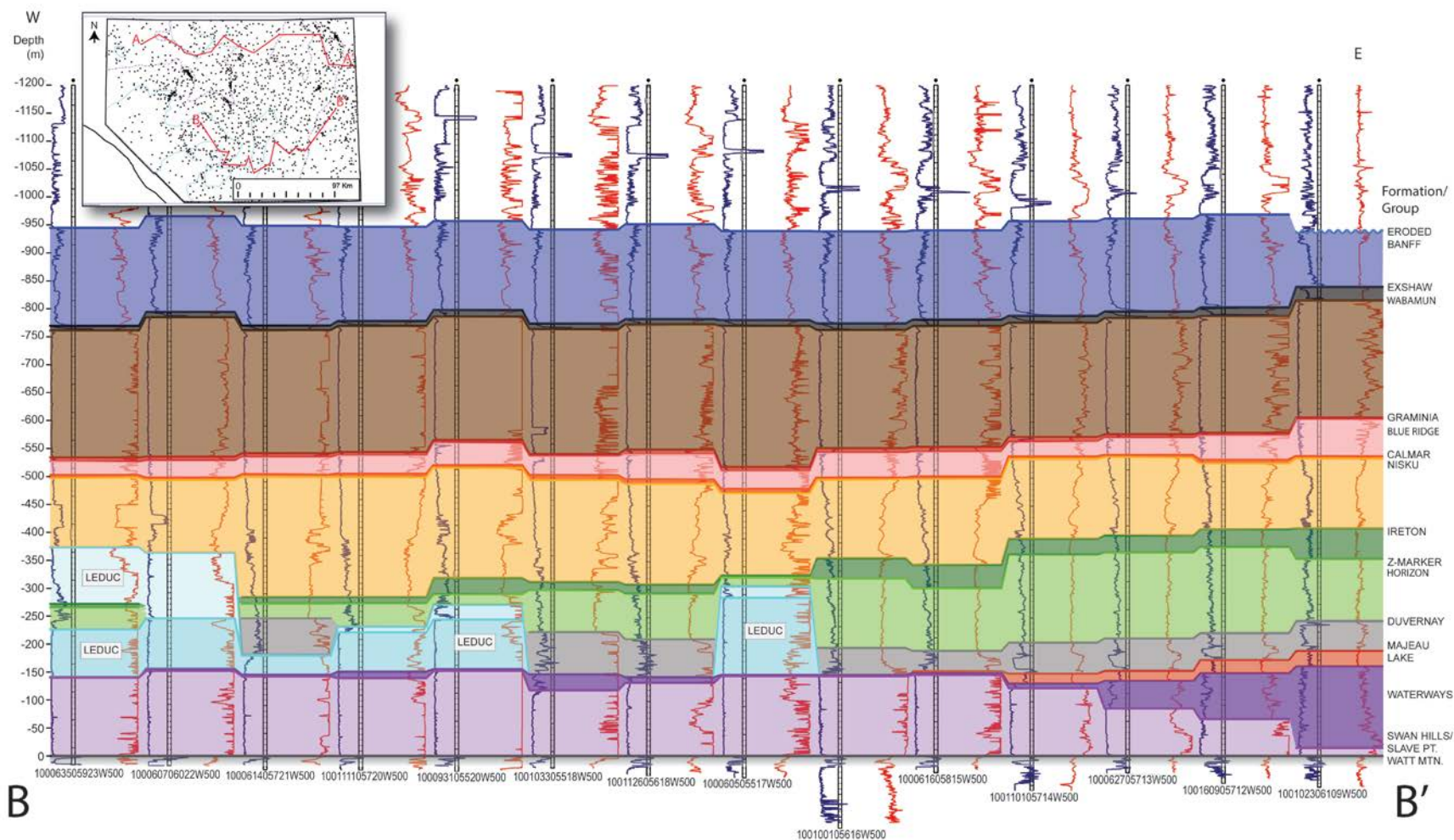


**Figure 8. Stratigraphic cross-section B–B' showing representative picks for the interval from the Watt Mountain Formation to the Banff Formation (Watt Mountain datum). Well-log traces include gamma ray (red) and resistivity (blue). Note the variable thickness of the Swan Hills, Slave Point, and Waterways formations. Inset map shows location of cross-section, west-central Alberta.**

## **4.4 Waterways Formation**

In the study area, the Waterways Formation is composed of argillaceous carbonate and calcareous shales that have been sourced from the east. Clinofolds from the east downlap onto the Slave Point Formation and Swan Hills Formation bank, and onlap the Swan Hills Formation reef margins in the areas where Leduc Formation reefs grew directly on top of the Swan Hills Formation reefs (Stoakes 1992a, b; Hauck 2014).

### **4.4.1 Stratigraphic Interval and Extent**

The Waterways Formation generally forms the top of the Beaverhill Lake Group in the study area, except in areas where the Leduc Formation reefs grew directly on top of the Swan Hills Formation reefs. Generally, in these areas, the Waterways Formation is not present. An example of one exception is well 06-14-069-20W5 (Figure 7), where the Majeau Lake Formation directly overlies the Swan Hills Formation reefs. Where the Waterways Formation is present, it is typically overlain by the Majeau Lake Formation.

### **4.4.2 Pick Criteria and Reference Wells**

The Waterways Formation was picked in 939 wells. The subsea depths for the pick dataset range from –1070.7 to –4013.6 m. Several cross-sections from Oldale and Munday (1994), Wendte and Uyeno (2005), and Hauck (2014) were used to correlate the top of the Waterways Formation. The picks in this dataset agree with the data in these publications for the study area. The top of the Waterways Formation was picked at the base of the Majeau Lake Formation. The transition into the Majeau Lake Formation is denoted by an increase in the measured gamma ray and a lower resistivity (Figures 7 and 8).

## **4.5 Majeau Lake Formation**

The Majeau Lake Formation of the Woodbend Group comprises basinal calcareous shale equivalent to the platform carbonates of the Cooking Lake Formation to the east (Stoakes, 1980; Stoakes, 1992a, b). The Majeau Lake Formation can be confused with the overlying Duvernay Formation due to similarity in lithology (calcareous shale). In drillcore, the colour of the Majeau Lake Formation is greenish-grey to black, differentiating it from the Duvernay Formation, which is a brownish-black to black shale. The Majeau Lake Formation, like the Duvernay Formation, is thought to have been deposited under low oxygen, and possibly euxinic, conditions (Stoakes, 1980).

### **4.5.1 Stratigraphic Interval and Extent**

The Majeau Lake Formation is present throughout the study area, except in the area where the Swan Hills Formation reef complex attains its greatest thickness. In this area, the Majeau Lake Formation appears to onlap the Swan Hills Formation reefs. A zero edge, indicating where the Majeau Lake Formation is not present, was used in the creation of the Majeau Lake Formation top surface within the 3D model. The Majeau Lake Formation overlies the Waterways Formation and is overlain by the Duvernay Formation.

### **4.5.2 Pick Criteria and Reference Wells**

The Majeau Lake Formation was picked in 760 wells. The subsea depths for the pick dataset range from –1012.1 to –3438.3 m. The top of the Majeau Lake Formation is marked by a distinguishing drop in resistivity that was used for correlation throughout the study area (Figures 7 and 8). Several publications were referenced during mapping within the Woodbend Group succession in west-central Alberta (Stoakes, 1980; Stoakes and Wendte, 1987; Stoakes, 1992a, b; Switzer et al., 1994).

## **4.6 Leduc Formation**

The Leduc Formation comprises a series of back-stepping carbonate platforms and isolated buildups that grew on top of the thickest accumulations of the underlying Swan Hills Formation reef complex (Stoakes, 1992a, b). The Leduc Formation can be divided into the lower Leduc Formation platform and the isolated and irregularly shaped upper Leduc Formation reefs. Many of the reefs and much of the platform in the Leduc Formation have been dolomitized producing mouldic and vuggy porosity (Green and Mountjoy, 2005).

### **4.6.1 Stratigraphic Interval and Extent**

In the study area, the Leduc Formation overlies thick portions of the Swan Hills Formation reefs. In some cases the Waterways Formation drapes the Swan Hills Formation reefs (Wendte and Uyeno, 2005). The Leduc reefs form a barrier around the Wild River sub-basin (Figure 4). Northeast of the Wild River sub-basin, there is a thick accumulation of the Leduc Formation that forms the Sturgeon Lake reef complex, which developed on top of the Snipe Lake reef complex of the Swan Hills Formation (Wendte and Uyeno, 2005).

The Leduc Formation reefs are overlapped by shales of the Duvernay and Ireton formations. The lower Leduc Formation platform, which represents shallow water carbonate deposition similar to the Cooking Lake Formation in the east, is draped by the Duvernay Formation in some areas within the Wild River sub-basin. In areas where the Ireton Formation shales do not overlie the Leduc Formation reefs, the Leduc Formation is directly overlain by the Nisku Formation.

### **4.6.2 Pick Criteria and Reference Wells**

The Leduc Formation was picked in 285 wells. The subsea depths for the pick dataset range from –1737.1 to –3953.6 m. The Leduc Formation top was picked using gamma-ray, resistivity, neutron porosity, and bulk density logs (Figures 7 and 8). The reefs of the Leduc Formation have a higher porosity than the reefs of the Swan Hills Formation and are often completely dolomitized. Neutron porosity and density logs also proved useful when distinguishing the top of Leduc Formation in places where Nisku Formation reefs overlie the Leduc Formation. There are slight differences in porosity and density between the Nisku Formation reefs and the Leduc Formation reefs.

## **4.7 Duvernay Formation**

The Duvernay Formation is composed of dark, organic-rich, laminated shale and has a variable thickness in west-central Alberta (Stoakes, 1992a, b). The Duvernay Formation was deposited in relatively deep water in sub-basins controlled by the distribution of Leduc Formation buildups that grew on the highs of the Swan Hills Formation reef complex (Stoakes and Creaney, 1984; Dunn et al., 2012). The Duvernay Formation can be recognized from the underlying shales of the Majeau Lake Formation by the dark brown and black organic-rich laminations, in contrast to the Majeau Lake Formation shales, which are slightly lighter in colour with a more grey-black colour. The overlying Ireton Formation shales are more calcareous than the Duvernay Formation shales and are greenish-grey (argillaceous) in colour with less pronounced laminations and a more massive or nodular appearance.

### **4.7.1 Stratigraphic Interval and Extent**

The Duvernay Formation was not deposited in areas where the Leduc Formation buildups are present, but can be found draping sections of the lower Leduc Formation platform. The Duvernay Formation is thickest in the west, surrounding the Wild River sub-basin and Leduc Formation reefs, and towards the east, where much of the argillaceous material in the Duvernay Formation was sourced (Stoakes and Wendte, 1987; Stoakes, 1992a, b). The Duvernay Formation generally overlies the Majeau Lake Formation, except where the Majeau Lake Formation is absent in the immediate vicinity of the Leduc

Formation reefs or where Duvernay Formation deposits drape the lower Leduc Formation platform. The Duvernay Formation is overlain by the Ireton Formation throughout the study area.

#### **4.7.2 Pick Criteria and Reference Wells**

The Duvernay Formation was picked in 814 wells. The subsea depths for the pick dataset range from -921.9 to -3942.0 m. The Duvernay Formation top was picked using gamma-ray and resistivity logs (Figures 7 and 8). The Duvernay Formation is marked by an increase in these log measurements compared to the overlying Ireton Formation and underlying Beaverhill Lake Group. Within the study area, the Duvernay Formation has a consistent resistivity 'shoulder' (Figures 7 and 8) that is not found elsewhere in Alberta. Formation tops were picked based on information from a variety of studies on Woodbend Group deposition (Stoakes, 1980; Stoakes and Wendte, 1987; Stoakes, 1992a, b; Switzer et al., 1994). These studies infer an easterly source for much of the siliciclastic material in the Duvernay Formation.

### **4.8 Ireton Formation and the Z-Marker Horizon**

The Ireton Formation comprises greenish- to dark-grey calcareous-rich shales that form clinoforms from east- to west-central Alberta. These shales are subdivided by the Z-marker horizon, an easily recognized marker bed that is considered to be part of the Woodbend Group but in more recent publications is referred to as marking the transition from Woodbend Group to Winterburn Group deposition (Stoakes, 1980; Stoakes, 1992a, b; Wendte et al., 1995; Atchley et al., 2018). The Z-marker is included as a horizon in the model because it is a widely used marker bed. Depositional patterns and thicknesses are drastically different between the Ireton Formation above and below the Z-marker horizon (Stoakes, 1992a, b).

#### **4.8.1 Stratigraphic Interval and Extent**

The Ireton Formation and Z-marker horizon are present throughout the basin, except in the areas where the Leduc Formation reefs have filled the accommodation space within the Woodbend Group. The Ireton Formation onlaps, and sometimes drapes, the Leduc Formation reefs in the Wild River sub-basin and in the northern part of the study area at the Sturgeon Lake reef complex. The Ireton Formation conformably overlies the Duvernay Formation and is conformably overlain by the Nisku Formation.

#### **4.8.2 Pick Criteria and Reference Wells**

The Z-marker horizon within the Ireton Formation was picked in 925 wells. The subsea depths for the pick dataset range from -888.2 to -3924.6 m. Subsea depths for the top of the Ireton Formation (picked in 964 wells) picks range from -706.3 to -3664.6 m. The Z-marker is easily distinguished by high gamma-ray readings and sonic interval transit time (Figures 7 and 8; Wendte et al., 1995). Reference wells from Wendte et al. (1995) were used to correlate the Z-marker horizon and the Ireton Formation. The Ireton Formation thins significantly in the Wild River sub-basin because of reduced sediment input from the east and several thick Leduc Formation reefs bordering the basin (Stoakes, 1980; Stoakes and Wendte, 1987; Stoakes 1992a, b; Wendte, 1998). Cross-sections by Wendte (1998) were also used to correlate the Ireton Formation top and Z-marker in this portion of the study area.

### **4.9 Nisku Formation**

The Nisku Formation is part of the Winterburn Group and was deposited during the Frasnian. In west-central Alberta, the Nisku Formation comprises five members: Wolf Lake, Cynthia, Bigoray, Lobstick, and Zeta Lake. These members represent diverse facies including slope and basinal carbonate rocks, shale, coral-algal and stromatoporoid biostromes, ramp carbonate rocks, and some peritidal carbonate rocks and evaporites (Watts, 1987). The transition from the underlying Ireton Formation to the Nisku Formation is gradational and facies overlap can be observed in the upper part of the Ireton Formation. Numerous lateral facies changes within the Nisku Formation render mapping in the subsurface by logs

alone a challenge. In areas of high complexity, such as the Wild River sub-basin, the individual members within the formation were used to help define the base and top of the Nisku Formation.

#### **4.9.1 Stratigraphic Interval and Extent**

The Nisku Formation is present throughout the study area. The thickest accumulation of the Nisku Formation is in the central part, southwestern corner, and Wild River sub-basin and surrounding area. There are numerous Nisku Formation reef buildups overlying the Leduc Formation reefs in the study area. The Nisku Formation conformably overlies the Ireton Formation and is overlain by the thin Calmar Formation. In the type well (L.S. 12, Sec. 25, Twp. 50, Rge. 26, W 4<sup>th</sup> Mer., abbreviated 12-25-050-26W4) of the Winterburn Group, the upper contact of the Nisku Formation with the overlying Calmar Formation appears to be karsted, but in much of the study area the contact is gradational. The contact appears variably erosional in areas where the Zeta Lake Member reefs are present (Wendte et al., 1995; McLean and Klapper, 1998).

#### **4.9.2 Pick Criteria and Reference Wells**

The Nisku Formation was picked in 1200 wells. The subsea depths for the pick dataset range from -661.7 to -3566.5 m. Gamma-ray, neutron porosity, bulk density, and resistivity wireline logs were used to correlate the Nisku Formation (Figures 7 and 8). Members of the Nisku Formation were mapped in the Wild River sub-basin area to help define the contact between the Nisku and Ireton formations (Wendte, 1998). In the southern portion of the study area, the Z-marker horizon was used as a guide to picking the contact between the Nisku and Ireton formations (Wendte et al., 1995). The Nisku Formation thins significantly in most of the northern portion of the study area, which allowed increased accommodation space for the overlying Blue Ridge Member of the Graminia Formation to be deposited.

### **4.10 Calmar Formation**

The Calmar Formation is part of the Winterburn Group. In west-central Alberta, the Calmar Formation is composed of mottled green and red siltstone and calcareous shale, and is, in some places, dolomitic or anhydritic (McLean and Klapper, 1998). In the Wild River sub-basin area, the Calmar Formation is conglomeratic with unsorted and subangular, greyish-green and reddish-brown mottled siltstone pebbles in a dolomitic siltstone matrix (Meijer Drees et al., 1998). There are areas of the study area, mostly in the deeper western portions of the Wild River sub-basin and Winterburn basin, where the Calmar Formation is difficult to distinguish from the Nisku and Graminia formations.

#### **4.10.1 Stratigraphic Interval and Extent**

The Calmar Formation has been mapped throughout the study area as a thin silty unit. It should be noted that in the middle of the study area, and in locations where the Nisku Formation shales onlap the Nisku Formation reefs, the Calmar Formation is not well defined and is particularly difficult to correlate (McLean and Klapper, 1998). In the area of Kaybob south (58-17W5) the contact with the underlying Nisku Formation is not conformable and the top of the Nisku Formation is karsted in some locations (Wendte et al., 1995; McLean and Klapper, 1998).

In some previous studies, the Calmar Formation is not distinguished from the overlying Graminia Formation but rather referred to as the “undifferentiated Winterburn shales” (Stoakes, 1992a, b; Wendte, 1998).

#### **4.10.2 Pick Criteria and Reference Wells**

The Calmar Formation was picked in 1196 wells. The subsea depths for the pick dataset range from -653.7 to -3560.6 m. The gamma-ray and photoelectric logs, and lithologs were used to correlate the Calmar Formation (Figures 7 and 8). Correlation was informed by a number of publications (which included cross-sections), especially for the contact between the Nisku and Calmar formations (Watts, 1987; Switzer et al., 1994; Meijer Drees et al., 1998; Wendte, 1998).

## **4.11 Graminia Formation**

The Graminia Formation consists of the lower Blue Ridge Member and the upper Graminia Silt Member. The Blue Ridge Member comprises three facies including a lower silty carbonate unit, a fossiliferous middle interval, and an upper interbedded silty and sandy unit (Meijer Drees et al., 1998). The Blue Ridge Member represents the last widespread carbonate cycle in the Frasnian (Switzer et al., 1994). The Graminia Silt Member comprises greenish-grey, reddish-brown, mottled silty carbonate rocks, and dolomitic siltstone and shale (Meijer Drees et al., 1998). Biostratigraphic ages derived from conodont data in age-equivalent strata in the Northwest Territories place the Graminia Silt Member in the Famennian (Geldsetzer, 1988; Switzer et al., 1994).

### **4.11.1 Stratigraphic Interval and Extent**

The Graminia Silt and Blue Ridge members of the Graminia Formation were mapped throughout the study area. The Blue Ridge Member conformably and gradationally overlies the Calmar Formation siltstone (Meijer Drees et al., 1998). The upper contact of the Blue Ridge Member is erosional and is overlain by siltstone and shale of the Graminia Silt Member. The Graminia Formation is overlain by carbonate rocks of the Wabamun Group. This contact is conformable and gradational because the upper part of the Graminia Formation was reworked during the transgression that took place at the beginning of the deposition of the Wabamun Group (Stoakes, 1992a, b). The thickness of the Graminia Silt Member is variable throughout the area but is always less than 10 m. The Blue Ridge Member thickens in the northern portion of the study area where the underlying Nisku Formation did not fill as much of the available accommodation space.

### **4.11.2 Pick Criteria and Reference Wells**

The Graminia Formation top (i.e., top of the Graminia Silt Member) was picked in 1231 wells. The subsea depths for the pick dataset range from -597.8 to -3521.7 m. The Blue Ridge Member was picked in 1227 wells. The subsea depths for this pick dataset range from -603.5 to -3521.8 m. Gamma-ray and resistivity logs were used to correlate these surfaces throughout the study area. The Graminia Silt Member is particularly easy to recognize using gamma-ray logs, as it is highly radioactive (Figures 7 and 8; Meijer Drees et al., 1998). Cross-sections in Meijer Drees et al. (1998) and Wendte (1998) were used as reference for correlation of the Graminia Formation and its members.

## **4.12 Wabamun Group**

In west-central Alberta, the Wabamun Group consists of the Stettler Formation and a thin, partially eroded Big Valley Formation (Halbertsma, 1994). The Wabamun Group represents carbonate deposition in a ramp setting at the close of the Devonian (Stoakes, 1992c). Predominantly composed of limestone, dolomite, and some anhydrite, the Wabamun Group is a thick succession deposited during an overall transgressive-regressive cycle (Stoakes, 1992a, b).

### **4.12.1 Stratigraphic Interval and Extent**

Strata of the Wabamun Group are present throughout the study area and overlie the Graminia Silt Member of the Graminia Formation. The top of the Wabamun Group is represented by the thin and partially eroded Big Valley Formation (cf. Halbertsma, 1994). The Big Valley Formation is overlain by the Exshaw Formation.

### **4.12.2 Pick Criteria and Reference Wells**

The Wabamun Group was picked in 1269 wells. The subsea depths for the pick dataset range from -347.92 to -3305.1 m. The Wabamun Group top was easily correlated throughout the study area using the gamma-ray log, which shows characteristically low readings due to the presence of clean limestone

and dolomite throughout the unit ([Figures 7 and 8](#)). Reference material for correlation was taken from Halbertsma (1994).

### **4.13 Exshaw Formation**

The Exshaw Formation is a thin marker bed that represents the transition from Devonian to Carboniferous deposition in the WCSB (Richards et al., 1994). The type section of Exshaw Formation comprises thin black fissile shale containing quartz silt, microcrystalline pyrite, and minor shelly fragments, overlain by a thicker unit of siltstone (~40 m; Macqueen and Sandberg, 1970; Meijer Drees and Johnston, 1993). The Exshaw Formation is easily recognized on well logs due to a highly radioactive gamma-ray log signature.

#### **4.13.1 Stratigraphic Interval and Extent**

The Exshaw Formation is present throughout the study area; however, the sub-Cretaceous unconformity truncates the Exshaw Formation immediately northeast of the study area. The Exshaw Formation overlies the Big Valley Formation of the Wabamun Group. The Exshaw Formation is overlain by siltstone, carbonate rocks, and shale of the Banff Formation.

#### **4.13.2 Pick Criteria and Reference Wells**

The Exshaw Formation was picked in 1264 wells. The subsea depths for the pick dataset range from -297.9 to -3296.4 m. The gamma-ray log can be used to recognize the base of the Exshaw Formation due to the highly radioactive nature of the shale at the base of the Exshaw Formation ([Figures 7 and 8](#)). The top of the Exshaw Formation was correlated using both gamma-ray and resistivity logs. The upper silty unit in the Exshaw Formation in this area was recognized using previously published cross-sections (Richards et al., 1994).

### **4.14 Banff Formation**

The Banff Formation consists of four informal members, A through D. All four members are present in most of the study area (Richards et al., 1994, Figure 14.26). The uppermost members are not present in the northeastern part of the study area where they have been eroded (associated with the sub-Cretaceous unconformity). Member A consists of a cleaning-upwards package of lime mudstone and shale, which gradationally transitions into member B, a cleaner limestone unit. Member C consists of mixed carbonate and fine-grained clastic rocks, locally containing anhydrite. Member D is mainly siltstone and is easily recognized due to increased radioactivity compared to the underlying carbonate-rich members. Deposition during this time took place in a carbonate ramp setting with some poorly defined carbonate platforms developing in a few areas (Richards et al., 1994).

#### **4.14.1 Stratigraphic Interval and Extent**

The Banff Formation is present throughout the study area but is partially eroded in the northeast at the sub-Cretaceous unconformity, where it is unconformably overlain by the Cretaceous Mannville Group. The Banff Formation conformably overlies the Exshaw Formation (Smith and Bustin, 2000) and is unconformably overlain by the Pekisko Formation in areas where it is not truncated by the sub-Cretaceous unconformity.

#### **4.14.2 Pick Criteria and Reference Wells**

The Banff Formation was picked in 1585 wells. The subsea depths for the pick dataset range from -115.1 to -3186.5 m. The pick dataset contains formation tops used to create the sub-Cretaceous unconformity surface (Peterson and MacCormack, 2014). Gamma-ray (a sharp decrease) and resistivity logs (an increase) were used to correlate the top of the Banff Formation throughout the study area ([Figures 7 and 8](#)).

## **4.15 Pekisko Formation**

The Pekisko Formation forms the base of the Rundle Group within the Peace River Embayment (O'Connell, 1990). It consists of massive, coarse-grained, echinodermal limestone deposited on a carbonate ramp during the Mississippian (O'Connell, 1990).

### **4.15.1 Stratigraphic Interval and Extent**

Within the study area, the Pekisko Formation unconformably overlies the Banff Formation. In the southern part of the study area, it is truncated by the sub-Jurassic unconformity, where it is overlain by the Nordegg Member of the Fernie Formation. In the northeast, the Pekisko Formation is truncated by the sub-Cretaceous unconformity, where it is overlain by the Cretaceous Gething Formation. Where the Pekisko Formation is uneroded (in the west), it is in conformable contact with the overlying Shunda Formation.

### **4.15.2 Reference Logs and Picking Criteria**

The Pekisko Formation was picked in 1335 wells. The subsea depths for the pick dataset range from -250.9 to -3192.0 m. This pick dataset contains formation tops used to create the sub-Cretaceous unconformity surface (Peterson and MacCormack, 2014). The type log used for picking is from Richards et al. (1994). Additionally, the works of Law (1981) and O'Connell (1990) were used. The top of the Pekisko Formation was picked at the gamma-ray marker visible in the type log of Richards et al. (1994; [Figures 9 and 10](#)). This is in disagreement with O'Connell (1990), who put the top above the gamma-ray marker, including the overlying shale in the Pekisko Formation. Richards et al. (1994) outlined the overlap of the Pekisko Formation stratotype (borehole 02-25-019-03W5) with the Shunda Formation and argued that, as the Shunda Formation was defined first and holds precedence, the Pekisko Formation should not include the upper shale. Instead, the shale should be included in the Shunda Formation (Richards et al., 1994). The upper shale was therefore not included in the Pekisko Formation in this model.

## **4.16 Shunda Formation**

The Shunda Formation consists of argillaceous micritic limestone and shale deposited within the Peace River Embayment (Law, 1981). The lower Shunda Formation comprises deposits formed during a regional transgression (Richards et al., 1994). A subsequent major regression, during the late Tournaisian, produced restricted-marine carbonate and anhydrite deposits (Richards et al., 1994).

### **4.16.1 Stratigraphic Interval and Extent**

The Shunda Formation forms part of the Rundle Group and conformably overlies the Pekisko Formation (Macauley, 1958). The Debolt Formation conformably overlies the Shunda Formation within the study area (Macauley, 1958). In the southeastern part of study area, the Shunda Formation is partially truncated by the sub-Jurassic unconformity, where it is overlain by the Nordegg Formation. The Shunda Formation is also truncated by the sub-Cretaceous unconformity, where it is overlain by the Cretaceous Gething Formation.

### **4.16.2 Reference Logs and Picking Criteria**

The Shunda Formation was picked in 997 wells. The subsea depths for the pick dataset range from -325.3 to -3104.5 m. The pick dataset contains formation tops used to create the sub-Cretaceous unconformity surface (Peterson and MacCormack, 2014). The type log used for picking is from Law (1981). Additionally, the works of Macauley (1958) and Richards et al. (1994) were used during the picking of the Shunda Formation. The top of the Shunda Formation was picked at the gamma-ray marker visible in the type log of Law (1981; [Figures 9 and 10](#)). This pick is in agreement with Richards et al. (1994).

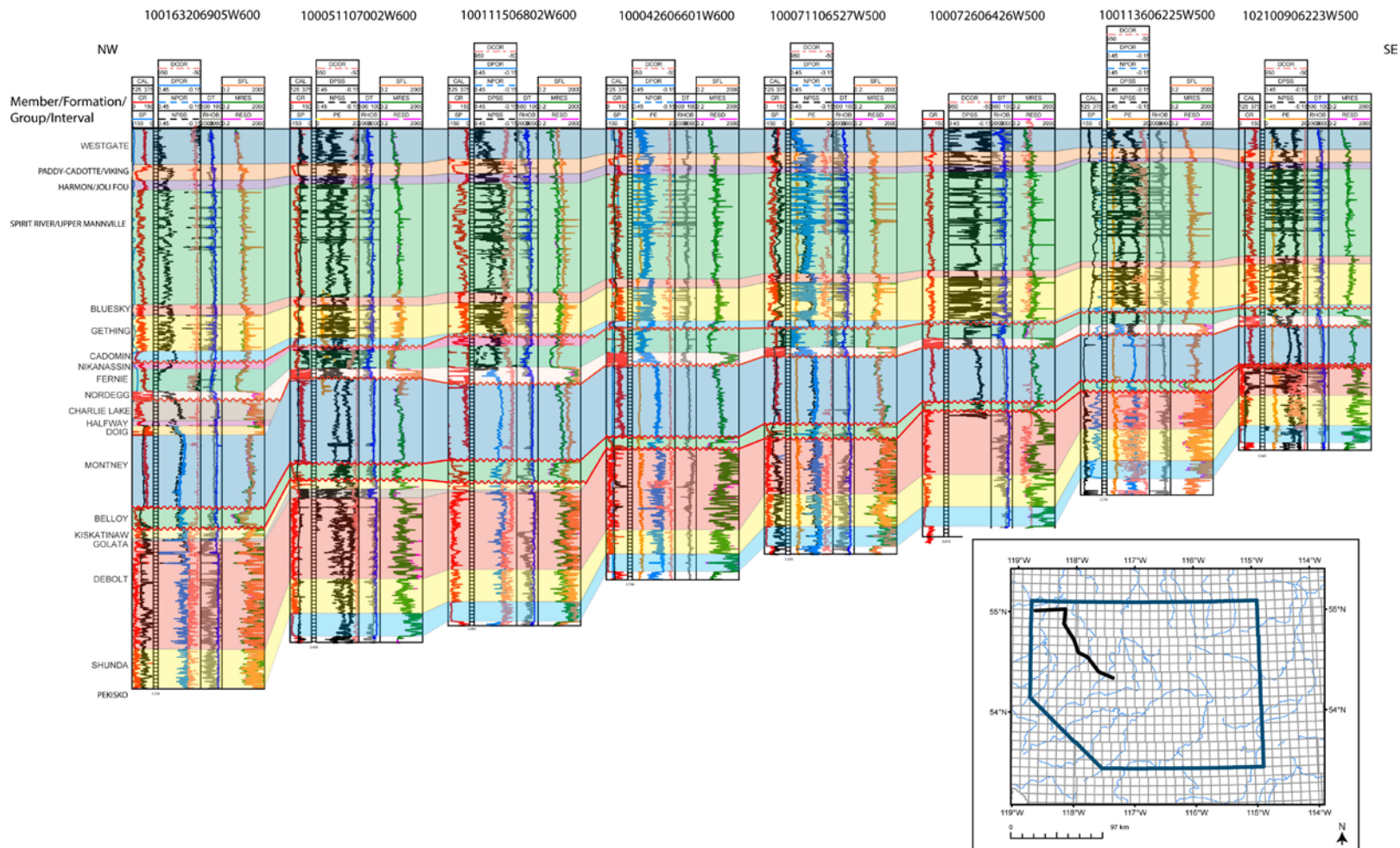


Figure 9. Stratigraphic cross-section showing representative picks for the interval from the Pekisko Formation to the base of the Fish Scales Formation. This section highlights the Upper Triassic interval in the northwest (NW) which becomes eroded away in the southeast (SE) portion of the study area. Log suites are separated into four tracks for each well: track one includes caliper (black), gamma ray (GR, red) and spontaneous potential (SP, blue) logs; track two includes density correction (DCOR, pink), density porosity (DPOR, blue), neutron porosity (NPOR, blue dotted) and neutron porosity on a sandstone scale (NPSS, black dotted); track three includes DT (blue) and RHOB (grey); track four includes shallow focussed laterolog (SFL, orange), medium resistivity (MRES, green), and deep resistivity (RESD, pink). Note also the four major unconformity surfaces included in the model (denoted by wavy lines). Inset map shows location of cross-section (black line), west-central Alberta.

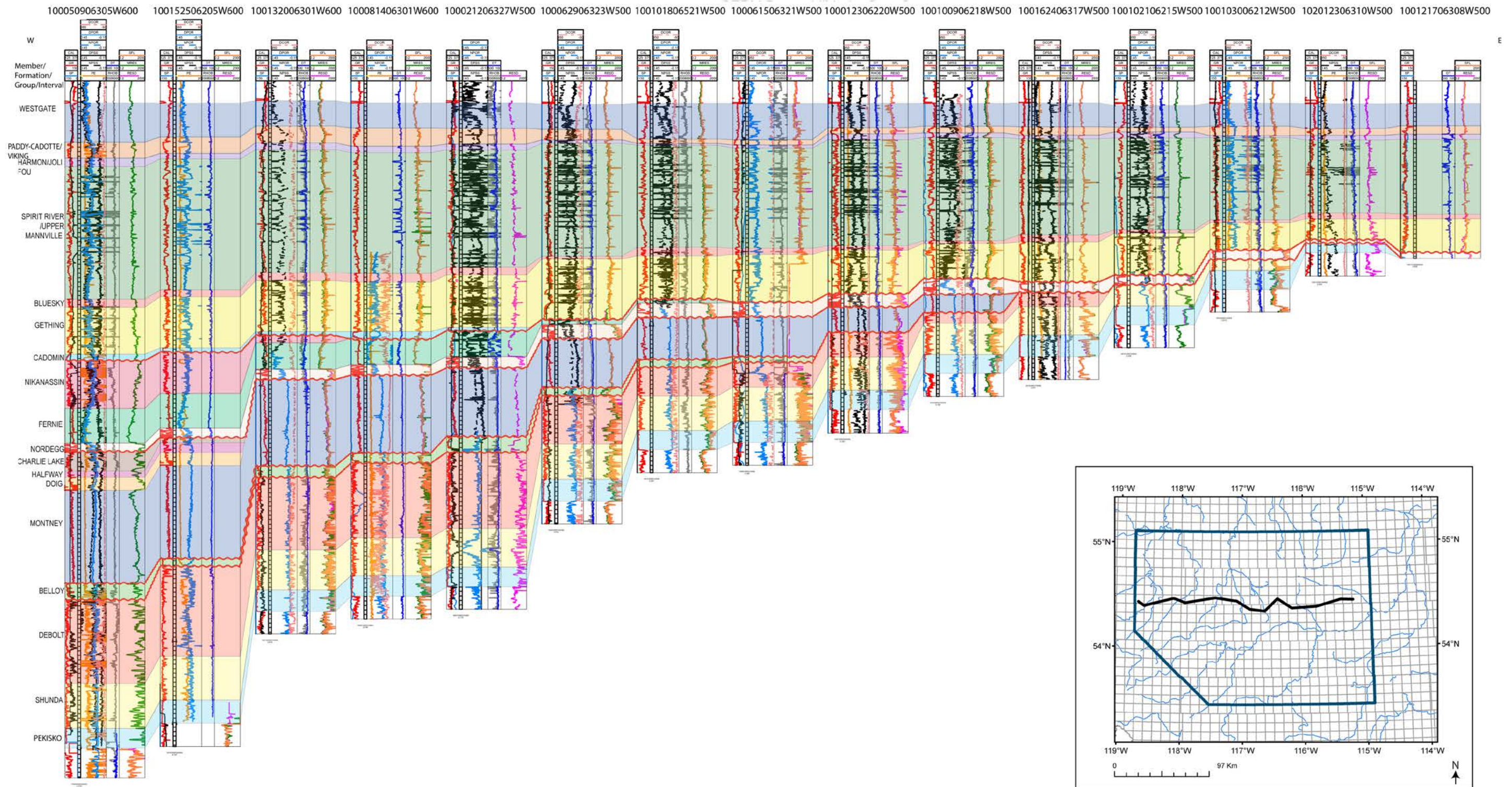


Figure 10. Stratigraphic cross-section showing representative picks for the interval from the Pekisko Formation to the base of the Fish Scales Formation (cross-section datum). Log suites are separated into four tracks for each well: track one includes caliper (black), gamma ray (GR, red) and spontaneous potential (SP, blue) logs; track two includes density correction (DCOR, pink), density porosity (DPOR, blue), neutron porosity (NPOR, blue dotted) and neutron porosity on a sandstone scale (NPSS, black dotted); track three includes DT (blue) and RHOB (grey); track four includes shallow focussed laterolog (SFL, orange), medium resistivity (MRES, green), and deep resistivity (RESO, pink). Highlighted is the merging relationship of the four major unconformities (the sub-Permian, sub-Triassic, sub-Jurassic, and sub-Cretaceous; shown by wavy lines), as well as the filling of the foredeep of the basin by the deposits above the sub-Cretaceous unconformity surface. Inset map shows location of cross-section (black line), west-central Alberta.

## **4.17 Debolt Formation**

The Debolt Formation was first defined by Macauley (1958). It is generally divisible into an upper and lower Debolt Formation (Macauley, 1958). The lower Debolt Formation consists of massive, brown, cherty, bioclastic limestone; the upper Debolt Formation is characterized by crystalline to massive dolostone with interbedded anhydrite (Macauley, 1958). These units have been further subdivided by Law (1981) into argillaceous and carbonate members.

### **4.17.1 Stratigraphic Interval and Extent**

In general, where the Debolt Formation is preserved it is conformably overlain by the Stoddart Group, particularly by the basal Golata Formation (Macauley, 1958). In the south-central basin of the Dawson Creek Graben Complex, where the Golata Formation is absent, the Debolt Formation is unconformably overlain by the Kiskatinaw Formation of the Stoddart Group (Barclay et al., 1990). The sub-Permian unconformity is marked where the Belloy Formation overlies the Debolt Formation in the west. Additionally, the Debolt Formation was eroded (associated with the sub-Triassic unconformity) where it underlies the Montney Formation in the middle of the study area. It was also eroded in the southeast (associated with the sub-Jurassic unconformity), where it is overlain by the Nordegg Member of the Fernie Formation. Finally, in the northeastern part of the study area, the Debolt Formation was eroded away at the sub-Cretaceous unconformity and is overlain by the Gething Formation ([Figure 11](#)).

### **4.17.2 Reference Logs and Picking Criteria**

The Debolt Formation was picked in 867 wells. This pick dataset contains formation tops used to create the sub-Cretaceous unconformity surface (Peterson and MacCormack, 2014). The subsea depths for the pick dataset range from -338.4 to -3026.2 m. The type log used for picking is from Barclay et al. (1990). Additionally, the works of Macauley (1958), Law (1981), and Richards et al. (1994) were referenced during the picking of the Debolt Formation. The Debolt Formation top was picked at the gamma-ray marker visible in the logs of Barclay et al. (1990; [Figures 9](#) and [10](#)). This pick is in agreement with Richards et al. (1994).

## **4.18 Stoddart Group**

The Carboniferous Stoddart Group comprises three formations: the Golata, Kiskatinaw, and Taylor Flat. The Stoddart Group marks a transition in the WCSB from carbonate (Rundle Group) to siliciclastic deposition (Barclay et al., 1990). The Golata Formation is the lowermost unit of the Stoddart Group and is dominated by shale deposits (Barclay et al., 1990). The Kiskatinaw Formation is the middle unit of the Stoddart Group and comprises thick sandstone units interbedded with shale (Halbertsma, 1959; Barclay et al., 1990). The Kiskatinaw Formation comprises transgressive fluvio-estuarine to shallow-marine deposits bearing a tidal signature (Barclay, 1989; Barclay and Davies, 1989; Richards, 1989; Barclay et al., 1990). The Taylor Flat Formation comprises calcareous and bioclastic sandstone, bioclastic sandy packstone to grainstone, and minor shale and dolostone (Barclay et al., 1990). The Taylor Flat Formation was likely deposited on a poorly developed carbonate ramp (Richards, 1989; Barclay et al., 1990).

### **4.18.1 Stratigraphic Interval and Extent**

The Golata Formation onlaps the upper Debolt Formation and was deposited in a shallow low-energy embayment (Richards, 1989; Barclay et al., 1990). Generally, the contact between the Golata Formation and the underlying Debolt Formation is conformable, except along the margins of the Golata Formation (Barclay et al., 1990). The Golata and Kiskatinaw formations are present within the northwestern corner of the study area. The Taylor Flat Formation is generally confined to graben boundary limits (Barclay et al., 1990), and was not found in the study area.

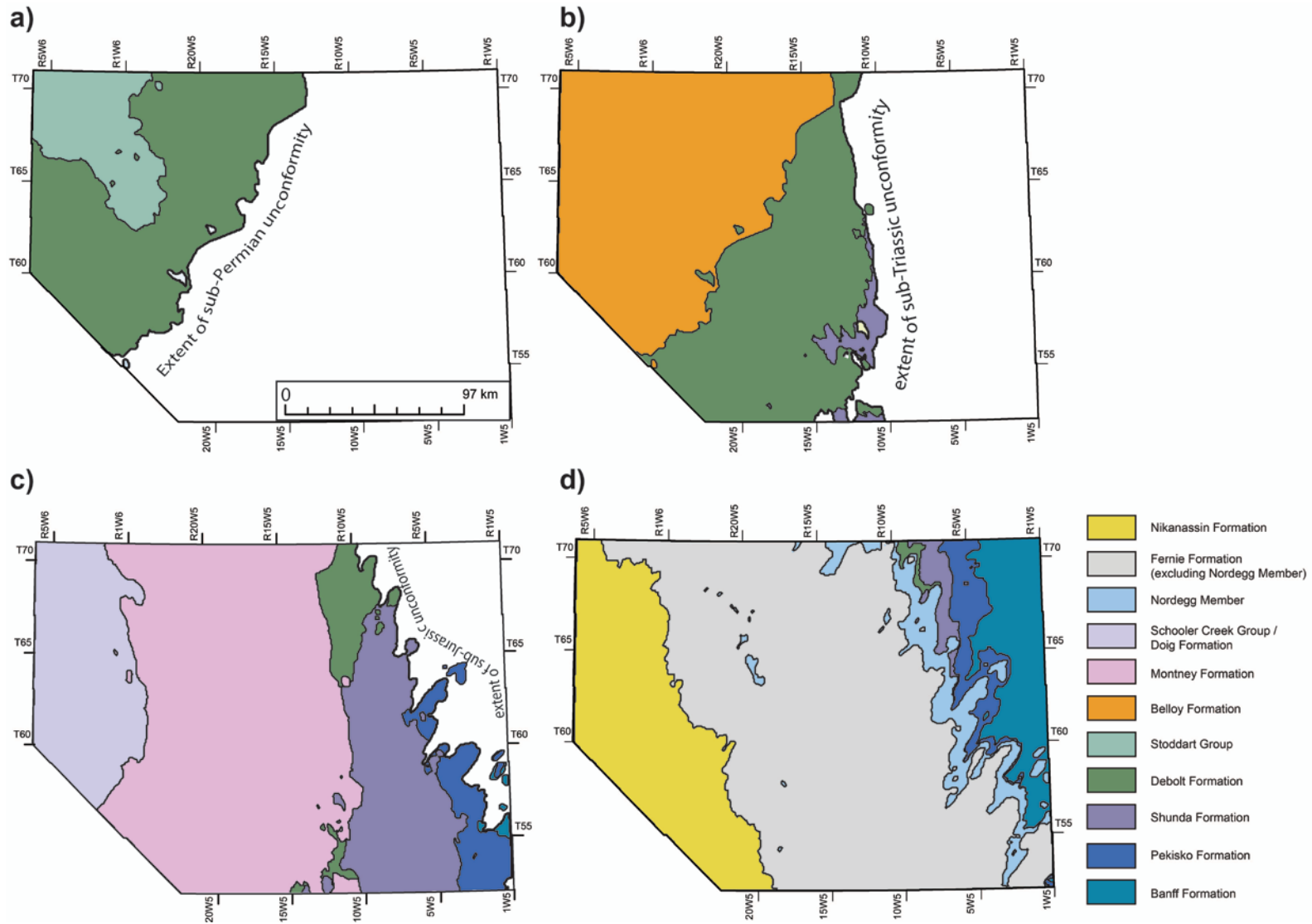


Figure 11. Two-dimensional maps of the unconformities in the west-central Alberta model. The coloured area represents the extent of the area affected by each unconformity in the 3D model: a) sub-Permian; b) sub-Triassic; c) sub-Jurassic; and d) sub-Cretaceous.

Because of the scarcity of available data points, surfaces for the individual formations were not created. Instead, data points from the uppermost Stoddart Group were combined to create a Stoddart Group surface. Because of erosion associated with the sub-Permian unconformity, this surface contains points from both the Kiskatinaw and Golata formations. The sub-Permian unconformity marks the contact between the Stoddart Group and the overlying Belloy Formation ([Figure 11](#)).

#### **4.18.2 Reference Logs and Picking Criteria**

The Stoddart Group was picked in 29 wells. The subsea depths for the pick dataset range from -1375.3 to -2013.7 m. The type log used for picking is from Barclay et al. (1990). Additionally, the works of Macauley (1958), Henderson et al. (1994), and Richards et al. (1994) were referenced during the picking of the Stoddart Group. The top of the Golata and Kiskatinaw formations were picked at gamma-ray markers visible in the logs of Barclay et al. (1990; [Figures 9 and 10](#)).

Barclay et al. (1990) differentiated Kiskatinaw Formation shale from overlying shales of the Taylor Flat or Belloy formations using sonic and porosity logs, observing that the Kiskatinaw Formation shale shows high porosity responses. The interbedded nature of the Kiskatinaw Formation also differentiates it from overlying units, contrasting with the relatively clean gamma-ray signature of the Belloy and Taylor Flat formations (Barclay et al., 1990). The Golata Formation displays high radioactivity on gamma-ray logs, positive spontaneous potential values, and low resistivity values (Halbertsma, 1959; Barclay et al., 1990).

### **4.19 Belloy Formation**

The Belloy Formation consists of mixed siliciclastic-carbonate deposits, including dolostone, sandstone, chert, and minor limestone and shale (Barclay et al., 1990). Henderson et al. (1994), in agreement with Halbertsma (1959), divided the Belloy Formation into three subdivisions (lower carbonate, middle sandstone, and upper sandstone units), separated by internal unconformities. Belloy Formation deposition has been interpreted to have been controlled by differential subsidence of horsts and grabens related to faulting in the Peace River Embayment (Barclay et al., 1990). Stratigraphic correlation over large distances is challenging because lithological trends and facies can be confined within depressions, and are not easily correlated across highs (Naqvi, 1972; Barclay et al., 1990).

#### **4.19.1 Stratigraphic Interval and Extent**

The Belloy Formation extends over roughly half of the northwestern part of the study area and overlies the Stoddart Group in the northwest and the Debolt Formation to the southeast and east ([Figure 11](#)). It is truncated by the sub-Triassic unconformity, where it is overlain by the Triassic Montney Formation. The Belloy Formation is differentiated from underlying units by the radioactive phosphatic shale and conglomerate deposits at the base of the formation (possibly basal lag deposits; Naqvi, 1972; Barclay et al., 1990).

#### **4.19.2 Reference Logs and Picking Criteria**

The Belloy Formation was picked in 662 wells. The subsea depths for the pick dataset range from -614.3 to -2979.0 m. The type log used for picking is from Barclay et al. (1990). Additionally, the works of Naqvi (1972) and Richards et al. (1994) were referenced during the picking of the Belloy Formation. The top of the Belloy Formation was picked at a pronounced gamma-ray marker visible in the logs of Barclay et al. (1990) at the unconformable contact with the overlying Montney Formation ([Figures 9 and 10](#)). However, the base of the Belloy Formation was more difficult to differentiate. The base of the Belloy was differentiated from the underlying Kiskatinaw and Golata Formations by gamma-ray signature, spontaneous potential, and resistivity changes after Halbertsma, (1959) and Barclay et al. (1990).

## **4.20 Montney Formation**

The Montney Formation was deposited in the Peace River Embayment during the Early Triassic (Davies, 1997). Lithological character varies from sandstone and siltstone to coquina (Zonneveld et al., 2010). With the exclusion of coquina deposits, grain size within the Montney Formation is generally restricted to the range of silt to very fine sand (Davies, 1997). Ichnological and sedimentological work suggests deposition occurred along a storm-influenced shoreface, which experienced periodic dysoxia (Zonneveld et al., 2010). Deposition occurred during faunal recovery following the mass extinction at the end of the Permian (Zonneveld et al., 2010).

### **4.20.1 Stratigraphic Interval and Extent**

Within the study area, the Montney Formation was progressively thinned by erosion at the sub-Jurassic unconformity eastward from the western edge of the study area until it pinches out midway through the study area (Figure 11). It is divided into three informal members: the lower member (Griesbachian to Dienerian age), Coquinal dolomite middle member (Dienerian to Smithian age), and upper member (Smithian to Spathian age; Davies, 1997).

### **4.20.2 Reference Logs and Picking Criteria**

The Montney Formation was picked in 2687 wells. The subsea depths for the pick dataset range from -610.7 to -2826.0 m. The type log used for picking is from Zonneveld et al. (2010). Additionally, the logs of Chalmers and Bustin (2012) were employed. The top of the Montney Formation was picked at the base of the Doig phosphate zone, where present (Figures 9 and 10). This is in agreement with Edwards et al. (1994). Elsewhere, where the Upper Triassic interval is absent, the top of the Montney Formation was picked at the highly radioactive base of the Jurassic Nordegg Member of the Fernie Formation (Figures 9 and 10).

## **4.21 Schooler Creek Group / Doig Formation Interval**

The Schooler Creek Group / Doig Formation interval contains a high diversity of lithologies ranging from sandstone to evaporites and carbonate rocks deposited in varying environments, such as tidal-marine channels and sabkha environments (Edwards et al., 1994). Within the Schooler Creek Group / Doig Formation interval, several unconformities are present, including at the bases of the Halfway and Charlie Lake formations, and within the Charlie Lake Formation (Edwards et al., 1994; Zonneveld et al., 2004).

### **4.21.1 Stratigraphic Interval and Extent**

Within the study area, the Schooler Creek Group / Doig Formation interval was progressively thinned by erosion at the sub-Jurassic unconformity from the northwestern edge of the study area until it pinches out in the upper northwestern corner (Figures 10 and 11). It comprises the Doig, Halfway and Charlie Lake formations. The Pardonet and Baldonnel formations are not present in the study area.

### **4.21.2 Reference Logs and Picking Criteria**

The Schooler Creek Group / Doig Formation interval top was picked in 134 wells. The subsea depths for the pick dataset range from -1156.2 to -2571.0 m. The type log used for picking is from Edwards et al. (1994). Additionally, the work of Zonneveld et al. (2004) was employed. The pick set used to generate the top surface consists of tops of both the Doig and Charlie Lake formations. As the Charlie Lake Formation was eroded (sub-Jurassic unconformity), the Doig Formation became exposed and was eventually eroded away. The top of the Schooler Creek Group / Doig Formation interval is marked by the highly radioactive base of the Jurassic Nordegg Member (Figures 9 and 10).

## **4.22 Nordegg Member**

The Nordegg Member of the Fernie Formation consists of calcareous shale and organic-rich argillaceous limestone (Riediger et al., 1990). Lower Jurassic in age, the Nordegg Member contains abundant phosphate and is highly radioactive in the western part of the study area (Riediger et al., 1990). Nordegg Member deposition is postulated to have occurred in a restricted basin where anoxia and hypersaline conditions existed (Riediger et al., 1990).

### **4.22.1 Stratigraphic Interval and Extent**

Within the study area, the Nordegg Member was progressively thinned by erosion at the sub-Cretaceous unconformity from the western edge of the study area until it pinches out in the upper northeastern corner (Figures 6 and 11). It forms the base of the Fernie Formation, unconformably overlying Triassic deposits in the west and Mississippian strata in the east.

### **4.22.2 Reference Logs and Picking Criteria**

The top of the Nordegg Member was picked in 2792 wells. This pick dataset contains formation tops also used to create the sub-Cretaceous unconformity surface (Peterson and MacCormack, 2014). The subsea depths for the pick dataset range from -84.4 to -2848.8 m. The Nordegg Member was mapped separately from the Fernie Formation because of its importance as an oil-prone interval. The type log used for mapping this interval is from Poulton et al. (1990). Additionally, the works of Poulton et al. (1994) and Riediger (2002) were consulted to inform the pick dataset. The top of the Nordegg Member was placed at a resistivity decrease that correlates with both the highly radioactive interval (west) and the blocky carbonate signature (southeast) on the gamma-ray logs (Figures 9 and 10). The top of the Nordegg Member includes both eroded (related to the sub-Cretaceous unconformity) and noneroded tops.

## **4.23 Fernie Formation**

The Fernie Formation is generally divided into an Upper and Middle Jurassic portion (interbedded sandstone and shale, including the Passage Beds, Rock Creek Member, and Niton Member), and a Lower Jurassic interval (Nordegg and Gordondale members, Poker Chip Shale; Poulton et al., 1990) which include carbonate and shale deposits. The Lower Jurassic interval consists of pre-orogenic platform limestones and shales deposited on a stable platform (Poulton et al., 1994). Deposition during the Middle Jurassic is thought to have been tectonically controlled, with paleotopography and subsidence influencing lateral variation in facies (Poulton et al., 1994). Upper Jurassic deposits comprise foredeep-fill (Poulton et al., 1994).

### **4.23.1 Stratigraphic Interval and Extent**

Within the study area, the Fernie Formation was progressively thinned by erosion at the sub-Cretaceous unconformity from the western edge of the study area until it pinches out in the upper northeastern corner (Figures 6 and 11).

### **4.23.2 Reference Logs and Picking Criteria**

The top of the Fernie Formation was picked in 2399 wells. This pick dataset contains formation tops also used to create the sub-Cretaceous unconformity surface (Peterson and MacCormack, 2014). The subsea depths for the pick dataset range from -465.9 to -2732.03 m. The type log used for mapping the top of the Fernie Formation is from Poulton et al. (1990). Additionally, the works of Poulton et al. (1994) and Riediger (2002) were consulted to inform the pick dataset. The top of the Fernie Formation was placed where a distinct increase in resistivity occurs, which correlates with the blocky gamma-ray signature of the overlying Nikanassin and Cadomin formations; this resistivity marker also distinguishes the Fernie Formation from the overlying Gething Formation (Figure 11). The top of the Fernie Formation includes both eroded (related to the sub-Cretaceous unconformity) and uneroded tops.

## **4.24 Nikanassin Formation**

The Upper Jurassic Nikanassin Formation (equivalent to the Minnes Group of Stott, 1967) contains interbedded sandstone, siltstone, and shale (Poulton et al., 1990). These deposits comprise numerous coarsening- and shallowing-upwards sequences (Poulton et al., 1994).

### **4.24.1 Stratigraphic Interval and Extent**

Within the study area, the Nikanassin Formation was progressively thinned by erosion at the sub-Cretaceous unconformity from the western edge of the study area (Figures 9 and 10). The formation pinches out in the northeastern portion of the study area and forms a sandstone wedge (Poulton et al., 1990; Figure 10).

### **4.24.2 Reference Logs and Picking Criteria**

The top of the Nikanassin Formation was picked in 335 wells. This pick dataset contains formation tops also used to create the sub-Cretaceous unconformity surface (Peterson and MacCormack, 2014). The subsea depths for the pick dataset range from -1088.1 to -2845.0 m. The type log used for mapping the top of the Nikanassin Formation is from Poulton et al. (1990). Additionally, the works of Poulton et al. (1994) and Riediger (2002) were consulted to inform the pick dataset. The top of the Nikanassin Formation was placed at a gamma-ray change that correlates with the blocky gamma-ray signature of the overlying Cadomin Formation in the west (Figures 9 and 10). All Nikanassin Formation tops are eroded (related to the sub-Cretaceous unconformity) within the study area (Figure 11).

## **4.25 Cadomin Formation**

The Cadomin Formation forms the base of the Bullhead Group. It predominantly comprises conglomerate and thickens westward, reaching reported thicknesses of 180 m (White and Leckie, 1999). Lower Cretaceous in age, the Cadomin Formation was deposited in association with a lull in the Columbian Orogeny, which resulted in the deposition of coarse clastic sediments into the foreland basin (Leckie and Cheel, 1997; White and Leckie, 1999).

### **4.25.1 Stratigraphic Interval and Extent**

Within the study area, the Cadomin Formation extends from the western edge of the study area and onlaps the Fox Creek Escarpment (Figure 6). The Cadomin Formation unconformably overlies the Nikanassin Formation and is unconformably overlain by the Gething Formation (Cant and Abrahamson, 1996).

### **4.25.2 Reference Logs and Picking Criteria**

The top of the Cadomin Formation was picked in 400 wells. The type log used for mapping the top of the Cadomin Formation is from Cant and Abrahamson (1996). Additionally, the works of Poulton et al. (1994) and White and Leckie (1999) were used to inform the pick dataset. The top of the Cadomin was placed at the gamma-ray change which marks the transition to the overlying Gething Formation (Figures 9 and 10). Difficulties were encountered in trying to differentiate the Cadomin Formation from basal Gething Formation channel sandstone, especially near the Fox Creek Escarpment.

## **4.26 Gething Formation / Ostracod Beds / Ellerslie Member Interval**

The Lower Cretaceous Gething Formation comprises a range of lithologies, including fine- to coarse-grained sandstone, siltstone, shale, coal, and chert pebble conglomerate (Gingras et al., 2010). It is interpreted as having been deposited in a marginal-marine or continental environment (Gingras et al., 2010). Paleotopography had a significant influence upon Lower Cretaceous deposition; the Gething Formation is interpreted to represent valley fill, deposited between highlands (Hayes et al., 1994). In the southeastern part of the study area, the Gething Formation transitions to the Ellerslie Member and

Ostracod Beds of the lower Mannville Group and was mapped together with these units in the model as the Gething Formation / Ostracod Beds / Ellerslie Member zone.

#### **4.26.1 Stratigraphic Interval and Extent**

The Gething Formation/ Ostracod Beds / Ellerslie Member interval is conformably and unconformably overlain by the Bluesky Formation and unconformably overlies the Cretaceous Cadomin Formation in the western part of the study area and Jurassic and Mississippian strata in the eastern part.

#### **4.26.2 Reference Logs and Picking Criteria**

The top of the Gething Formation was picked in 851 wells. The subsea depths for the pick dataset range from -147.6 to -2491.8 m. The type log used for picking the Gething Formation is from Casas and Walker (1997), wherein the transition between the Gething and Bluesky formations is marked by a sharp, blocky decrease in the gamma-ray signature and a lack of coal markers (Figures 9 and 10). Additionally, the works of O'Connell (1988), Hayes et al. (1994), and Cant and Abrahamson (1996) were consulted to inform the pick dataset.

### **4.27 Bluesky Formation**

The Bluesky Formation is a heterolithic sand-dominated interval that forms part of a third-order transgressive systems tract (Mackay and Dalrymple, 2011). Bluesky Formation deposits were emplaced during flooding of drainage systems with a northwestward drainage path, emptying into the Cretaceous Boreal Sea of the WCSB (O'Connell, 1988; Cant and Abrahamson, 1996; Mackay and Dalrymple, 2011). The Bluesky Formation is interpreted as having been deposited in a wave-dominated estuarine environment (Hubbard et al., 2004)

#### **4.27.1 Stratigraphic Interval and Extent**

The Bluesky Formation conformably overlies the Gething Formation and, in the study area, is conformably overlain by the Wilrich Member of the Spirit River Formation. The Bluesky Formation covers the entire study area, but is thin and shows some small areas of depositional pinchout.

#### **4.27.2 Reference Logs and Picking Criteria**

The top of the Bluesky Formation was picked in 770 wells. The subsea depths for the pick dataset range from -142.9 to -2483.4 m. The type log used for picking the Bluesky Formation is from Casas and Walker (1997), wherein the transition from the Bluesky Formation to the Wilrich Member is marked by a sharp increase in the gamma-ray signature, giving the Bluesky Formation a blocky appearance on gamma-ray logs (Figures 9 and 10). Additionally, the works of O'Connell (1988), Hayes et al. (1994), Cant and Abrahamson (1996), Hubbard et al. (2002), Hubbard et al. (2004), and Mackay and Dalrymple (2011) were consulted to inform the pick dataset.

### **4.28 Spirit River Formation / Upper Mannville Group Interval**

The Spirit River Formation is found in the northern part of the study area and is correlative with strata of the upper Mannville Group found in the southeastern part of the study area. The Spirit River Formation is early Albian in age and consists of fine-grained, well-sorted sandstone, conglomerate, carbonaceous mudstone, and coal forming a clastic wedge (Cant, 1984). Deposition prograded into an epeiric sea within the Alberta Basin, with eight major transgressive and regressive sequences apparent (Cant, 1984). Each sequence is interpreted to represent beach and shoreface deposits overlain by backswamp and lagoonal sediments (Cant, 1984). The upper Mannville Group consists of marginal-marine and coal-bearing nonmarine deposits in central Alberta (Wadsworth et al., 2002).

#### **4.28.1 Stratigraphic Interval and Extent**

The Spirit River Formation is subdivided into the Wilrich, Falher and Notikewin members (Smith et al. 1984; Casas and Walker, 1997). Within the study area, the Spirit River Formation / upper Mannville Group interval conformably overlies the Bluesky and Gething formations, and is disconformably overlain by the Harmon Member / Joli Fou Formation interval.

#### **4.28.2 Reference Logs and Picking Criteria**

The top of the Spirit River Formation / upper Mannville Group interval was picked in 699 wells. The subsea depths for the pick dataset range from 80.9 to -2109.1 m. The type log used for picking the top of the interval is from Casas and Walker (1997), wherein the contact between the Spirit River Formation / upper Mannville Group interval and the Joli Fou Formation / Harmon Member interval is marked by a sharp increase in the gamma-ray signature (Figures 9 and 10). Additionally, the works of Cant (1984), Hayes et al. (1994), and Armitage et al. (2004) were consulted to inform the pick dataset.

### **4.29 Harmon Member / Joli Fou Formation Interval**

The middle Albian Harmon Member of the Peace River Formation (Fort St. John Group) and the late Albian Joli Fou Formation (Colorado Group), both consist largely of marine mudstone (e.g., Leckie et al., 2000). Although the two units are not stratigraphically correlative, they can be considered as a combined, mappable interval at a regional scale, and have been mapped as such in this study.

#### **4.29.1 Stratigraphic Interval and Extent**

The Harmon Member overlies the Spirit River Formation in the northwestern part of the study area, and the Joli Fou Formation overlies upper Mannville Group strata to the southeast. The Harmon Member is overlain by the Cadotte and Paddy members of the Peace River Formation, and the Joli Fou Formation is overlain by the Viking Formation. The combined Joli Fou Formation / Harmon Member interval extends across the entire study area.

#### **4.29.2 Reference Logs and Picking Criteria**

The top of the Joli Fou Formation / Harmon Member interval was picked in 672 wells. Subsea depths for the pick dataset range from 92.9 to -2103.1 m. The type log used for picking the top of the interval is from Reinson et al. (1994), wherein the contact between the Joli Fou Formation / Harmon Member interval and the overlying Paddy-Cadotte members / Viking Formation interval is marked by a sharp decrease in resistivity, as noted by Webb et al. (2005; Figures 9 and 10). Additionally, the work of Putnam and Ward (2001) was consulted to inform the pick dataset.

### **4.30 Viking Formation / Peace River Formation (excluding Harmon Member) Interval**

In this study, the sandstone-dominated Viking Formation and the sandstone-dominated Paddy and Cadotte members of the Peace River Formation have been mapped as a single combined interval. Relationships between these Albian units are complex, but the tops of the Viking Formation and Paddy Member are generally considered to be correlative (e.g., Leckie et al., 2000; Dafoe et al., 2010).

#### **4.30.1 Stratigraphic Interval and Extent**

The Viking Formation overlies the Joli Fou Formation in the southeastern portion of the study area, and the Paddy and Cadotte members overlie the Harmon Member to the northwest. The combined interval extends over the entire study area and is overlain by the Westgate Formation in the southeast and by correlative lower Shaftesbury Formation strata to the northwest (Leckie et al., 2000).

### **4.30.2 Reference Logs and Picking Criteria**

The top of the Viking Formation / Peace River Formation (excluding Harmon Member) interval was picked in 685 wells. Subsea depths for the pick dataset range from 115.2 to -2099.2 m. The type log used for picking the top of the interval is from Reinson et al. (1994), wherein the contact between the Viking Formation and the overlying Westgate or lower Shaftesbury Formation (the tops of which are denoted by the Base of Fish Scales marker) is marked by a sharp increase in gamma-ray readings, marking the transition from sandstone or silty sandstone to shale (Reinson et al., 1994; [Figures 9 and 10](#)). The work of Putnam and Ward (2001) was also consulted to inform the pick dataset.

### **4.31 Base of Fish Scales Marker**

The Base of Fish Scales marker is generally considered to mark the Albian–Cenomanian boundary (e.g., Bloch et al., 1993). It defines the top of the lower part of the Shaftesbury Formation (Fort St. John Group) where the overlying Dunvegan Formation is present, or the top of the Westgate Formation (Colorado Group) where the Dunvegan Formation is absent (Bloch et al., 1993). Both of these intervals are mudstone dominated.

#### **4.31.1 Stratigraphic Interval and Extent**

The Base of Fish Scales marker is a prominent regional marker that is continuous across the study area. It is overlain by highly radioactive laminated shale, bioclastic sandstone, and bentonite of the Fish Scales Member (upper Shaftesbury Formation) or Fish Scales Formation (Colorado Group; Bloch et al., 1993).

#### **4.31.2 Reference Logs and Picking Criteria**

The Base of Fish Scales marker was picked in 1987 wells. Subsea depths for the pick dataset range from 151.5 to -2148.0 m. The contact is typically marked by a sharp deflection to the right on both gamma-ray and resistivity logs ([Figures 9 and 10](#)). The type wells and cross-sections of Bhattacharya (1994) and Reinson et al. (1994) informed the correlation of this unit.

### **4.32 Belle Fourche Formation / Upper Shaftesbury Formation / Lower Kaskapau Formation Interval**

The mudstone-dominated, lower Cenomanian interval between the Base of Fish Scales marker and the base of the Dunvegan Formation is assigned to the upper Shaftesbury Formation. The upper boundary, which marks the top of the Fort St. John Group (Glass, 1990, p. 243), is placed at the base of the lowermost significant sandstone interval (Dunvegan Formation) overlying Shaftesbury Formation shale. Where present, the Dunvegan Formation splits the strata equivalent to the Fish Scales and Belle Fourche formations of the Colorado Group into the upper Shaftesbury Formation (Fort St. John Group) below and the Kaskapau Formation (Smoky Group) above ([Figure 12a](#)). The base of the Second White Specks Formation demarcates the top of the Belle Fourche Formation, where the Dunvegan Formation is absent, and extends as a log marker into the lower part of the Kaskapau Formation above the Dunvegan Formation. The Belle Fourche Formation consists of predominantly noncalcareous shale, siltstone, and bentonite forming a series of stacked coarsening-upwards cycles that coarsen upwards overall (Tu et al., 2007). For modelling purposes the shale interval enveloping the Dunvegan Formation was split into a Belle Fourche Formation / upper Shaftesbury Formation model zone and a lower Kaskapau Formation model zone (see [Section 3.3.2](#); [Figure 5](#)).

#### **4.32.1 Stratigraphic Interval and Extent**

The lithostratigraphic contact between the upper Shaftesbury Formation and the Dunvegan Formation is time-transgressive, stepping up through a series of offlapping, shingled units (sandy delta lobes) from northwest to southeast (e.g., Bhattacharya, 1994).

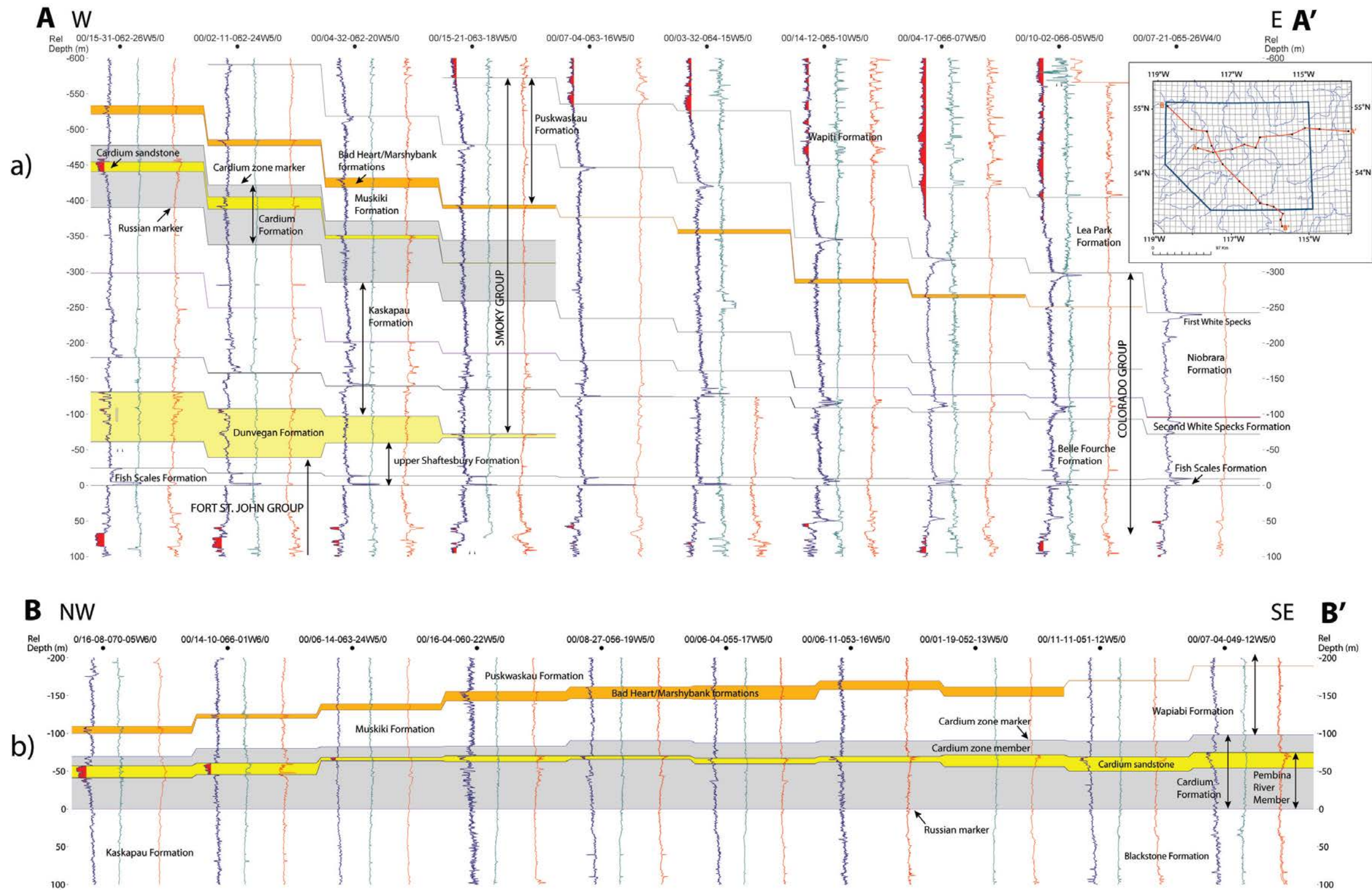


Figure 12. Stratigraphic cross-sections A–A' and B–B'. a) A–A' shows representative picks for the interval from the base of the Fish Scales Formation (cross-section datum) to the base of the Wapiti Formation. Note transition from Fort St. John Group, Dunvegan Formation, and Smoky Group to Colorado Group lithostratigraphic terminology from west to east. Colorado Group picks for well 07-21-065-26W4 (on the right) follow Tu et al. (2007, Figure 8 cross-section). Well logs are gamma-ray (blue line on the left, with red fill to left of 75 API cutoff), sonic (green line in the centre), and resistivity (red line on the right). b) B–B' shows representative picks for the Cardium Formation and Bad Heart / Marshybank formations. Datum is the Russian marker at the base of the Cardium Formation, with the Krause et al. (1994) reference well 07-04-049-12W5 at right. Well logs are gamma ray (blue line on the left, with red fill to left of 75 API cutoff), sonic (green line in the centre), and resistivity (red line on the right). Inset map shows location of cross-sections (red lines), west-central Alberta. Abbreviation: Rel, relative.

Southeast of the limit of the Dunvegan Formation (see below), strata correlative with the upper Shaftesbury Formation are included in the Fish Scales Formation and the lower part of the Belle Fourche Formation of the Colorado Group (Bloch et al., 1993). The top of the Cenomanian Belle Fourche Formation of the Colorado Group (Bloch et al., 1993) can be traced across the study area to southeast of the limit of the Dunvegan Formation. Where the underlying Dunvegan Formation is present, the base of the Second White Specks Formation forms a log marker within the Kaskapau Formation of the Smoky Group) (Figure 12a).

#### **4.32.2 Reference Logs and Picking Criteria**

The top of the Shaftesbury Formation was picked in 3015 wells with reference to type wells and cross-sections in Bhattacharya (1994). Subsea depths range from 785.2 to -1960.5 m. The top of the Belle Fourche Formation (and correlative lower Kaskapau Formation top) was picked in 1767 wells. Subsea depths range from 356.0 to -1817.5 m. Although there are minor differences in interpretation within this composite dataset, these picks are broadly consistent with those made by Tu et al. (2007, Figure 8 cross-section), and Bloch et al. (1993, Figure 7; well 10-21-055-25W4) to the east of the study area. The formation top is generally picked at the top of an interval that becomes siltier upward (decreasing gamma-ray reading) and is beneath the more radioactive shale and bioclastic sandstone of the Second White Specks Formation (Figure 12a).

### **4.33 Dunvegan Formation**

In the study area, the middle Cenomanian Dunvegan Formation forms a southeastward thinning clastic wedge consisting of interbedded mudstone, siltstone, and sandstone (e.g., Bhattacharya, 1994). Like the lower boundary (see upper Shaftesbury Formation above), the upper boundary of the Dunvegan Formation is highly diachronous.

#### **4.33.1 Stratigraphic Interval and Extent**

The top of the Dunvegan Formation is placed at the top of the uppermost significant sandstone interval underlying shale of the Kaskapau Formation, and marks the base of the Smoky Group. Dunvegan Formation sandstone intervals thin and eventually pass to shale at the southeastern definable limit of the formation (Figure 12a) beyond which correlative strata are included in the Belle Fourche Formation of the Colorado Group.

#### **4.33.2 Reference Logs and Picking Criteria**

The Dunvegan Formation was picked in 1982 wells, with reference to type wells and cross-sections in Bhattacharya (1994). Subsea depths range from 847.7 to -1862.7 m.

### **4.34 Second White Specks Formation**

The Second White Specks Formation consists mostly of calcareous shale and siltstone, with minor bioclastic sandstone and bentonite (Bloch et al., 1993; Tu et al., 2007).

#### **4.34.1 Stratigraphic Interval and Extent**

The top of the Cenomanian–Turonian Second White Specks Formation of the Colorado Group (Bloch et al., 1993) can be traced across the study area, southeast of the limit of the Dunvegan Formation. Where the underlying Dunvegan Formation is present, the top of the Second White Specks Formation forms a log marker at the top of a more radioactive shale interval (Figure 12a; Second White Speckled Shale of Plint, 2000, and Varban and Plint, 2005) within the mudstone-dominated Kaskapau Formation of the

Smoky Group. The shale interval between the top of the Second White Specks Formation and correlative log marker within the Kaskapau Formation and the base of the Cardium Formation (i.e., Russian marker, see [Section 4.35.1](#)) is referred to as the Blackstone Formation / middle Kaskapau Formation zone in the model.

#### **4.34.2 Reference Logs and Picking Criteria**

The Second White Specks Formation was picked in 808 wells. Subsea depths range from 377.5 to -1590.3 m. These picks are generally consistent with those made by Tu et al. (2007, Figure 8 cross-section) to the east of the study area, with the formation top typically marked by an upward decrease in resistivity accompanied by a variable, but commonly upward-increasing, gamma-ray response ([Figure 12a](#)).

### **4.35 Cardium Formation**

The muddy, sandy, and locally conglomeratic Cardium Formation forms an eastward-fining clastic wedge that was deposited along the western margin of the Alberta foreland basin in Turonian–Coniacian time. It is underlain by shale of the Kaskapau or Blackstone Formation and overlain by shale assigned to the Muskiki or Wapiabi Formation (Krause et al., 1994).

#### **4.35.1 Stratigraphic Interval and Extent**

The Cardium Formation is defined and subdivided using the lithostratigraphic scheme proposed for the central Alberta subsurface by Krause and Nelson (1984; see also Krause et al. 1994), based on their work in the Pembina oil field immediately south of the study area (northern limit of the field reaches the southeastern edge of the study area). Those authors divided the Cardium Formation into a lower Pembina River Member and an upper Cardium Zone Member. The base of the Cardium Formation is defined by the Russian marker (Krause et al., 1994, p. 379) and can be traced throughout the study area. At the top of the formation is the Cardium Zone marker, which loses definition and cannot be consistently picked to the east. The eastern extent of those picks is considered here to define the limit of the Cardium Formation. The upper portion of the Pembina River Member includes the Cardium sandstone, which is an easily correlatable lithostratigraphic unit.

#### **4.35.2 Pick Criteria and Reference Wells**

The following picks were made for this stratigraphic interval: 1) Russian marker in 1090 wells, subsea depth range from 392.1 to -1641.7 m; 2) Cardium sandstone base in 605 wells, subsea depth range from 69.6 to -1521.4 m; 3) Cardium sandstone top (Pembina River Member top) in 652 wells, subsea depth range from 71.7 to -1596.1 m; 4) Cardium Zone marker (Cardium Formation top) in 823 wells, subsea depth range from 389.4 to -1450.7 m.

In this study, picks were made for the basal Russian marker resistivity shoulder ([Figure 12a, b](#)); the Cardium Zone marker at the top of the Cardium Formation; and the top of the Cardium sandstone (top of Pembina River Member), using reference well 07-04-049-12W5 of Krause et al. (1994, p. 378, Figure 23.5) as a starting point (pick criteria are shown in [Figure 12](#)). An additional Cardium sandstone base pick was made to divide the upper, sandier part of the Pembina River Member from the finer grained lower part, using upward deflections to the left and right on gamma-ray and resistivity logs respectively. The Cardium sandstone interval is not present in the northeastern part of the study area.

### **4.36 Muskiki Formation / Upper Kaskapau Formation Interval**

The Muskiki Formation (Turonian–Coniacian) and correlative upper Kaskapau Formation strata consist mainly of mudstone and siltstone (Stott, 1963; Plint, 1990).

#### **4.36.1 Stratigraphic Interval and Extent**

The top of the Muskiki Formation (Stott, 1967) is placed at the base of the overlying siltstone and sandstone of the Marshybank Formation in the western and southwestern parts of the study area, and at the base of the younger Bad Heart Formation sandstone in the northeast (Plint, 1990). In the eastern part of the study area, the Muskiki Formation is not differentiated and the Kaskapau Formation extends up to the base of the Bad Heart Formation / Marshybank Formation interval.

#### **4.36.2 Pick Criteria and Reference Wells**

The top of the Muskiki Formation / upper Kaskapau Formation interval was picked in 899 wells, with subsea depths ranging from 421.5 to -1517.9 m. It was picked at the marked leftward deflection (increasing sand content upwards) of the gamma-ray log at the top of the shale succession, marking the base of the overlying Bad Heart and Marshybank formations ([Figure 12](#); Plint et al., 1990).

### **4.37 Lower Puskwaskau Formation / Bad Heart Formation / Marshybank Formation Interval**

The upper part of the Colorado Group and the correlative interval in the Smoky Group are mudstone-dominated and include the lower part of the Puskwaskau Formation. Within the model, this represents the volume from the base of the Bad Heart / Marshybank formations to the base of the Lea Park Formation and is referred to as the lower Puskwaskau Formation / Bad Heart Formation model zone.

#### **4.37.1 Stratigraphic Interval and Extent**

In the southeastern part of the study area, where the underlying Dunvegan Formation is absent, the top of the Santonian First White Specks Member of the Niobrara Formation marks the top of the Colorado Group shale succession (e.g., Tu et al., 2007) and the base of the Lea Park Formation. Where the Dunvegan Formation is present, the equivalent of the top of the Colorado Group within the Smoky Group forms a log marker (First White Specks Member top equivalent) within the Puskwaskau Formation ([Figure 12a](#)).

#### **4.37.2 Pick Criteria and Reference Wells**

The top of the Colorado Group and correlative log marker within the Puskwaskau Formation was picked in 1567 wells, with subsea depths ranging from 474.8 to -1045.6 m. The contact to the overlying upper Puskwaskau and Lea Park formations is characterized by a distinct upward decrease in gamma-ray readings, accompanied in the southeast by a decrease in resistivity ([Figure 12a](#)).

### **4.38 Lea Park Formation / Upper Puskwaskau Formation Interval**

These two formations consist largely of mudstone. Their tops represent the boundary between marine and overlying nonmarine deposits in the Upper Cretaceous succession

#### **4.38.1 Stratigraphic Interval and Extent**

The top of the Santonian–Campanian Puskwaskau Formation (Smoky Group: Stott, 1967; Hu and Plint, 2009) and the correlative top of the Lea Park Formation mudstone to the southeast mark the base of the Wapiti Formation ([Figure 12a](#)). Close to the foothills in the southwestern part of the study area where the Dunvegan Formation is absent, the mudstone-dominated succession from the top of the Cardium Formation to the base of the Wapiti/Brazeau formations is assigned to the Wapiabi Formation (Stott, 1963; Glass 1990, p. 670).

#### **4.38.2 Pick Criteria and Reference Wells**

Fanti and Catuneanu (2009, p. 272) placed this conformable contact at the base of the first laterally persistent coal seam that occurs at the top of the transitional and deltaic deposits belonging to the

Puskwaskau Formation, and provided type wells and cross-sections. Picks for this surface form a subset of the wider dataset published by Glombick (2013) and include data from 1602 wells with an approximate subsea depth range of 375 m to 950 m.

#### **4.39 Wapiti Formation**

The nonmarine, Campanian–Maastrichtian Wapiti Formation consists of fluvial deposits, coal seams, and subordinate lacustrine deposits (Fanti and Catuneanu, 2009).

##### **4.39.1 Stratigraphic Interval and Extent**

In the study area, the Wapiti Formation is overlain by the relatively thin (0 to 18 m), mudstone-dominated Battle Formation (Figure 13), except in the Edson–Whitecourt area (Hathway, 2011a, b) where the Battle Formation has been removed by erosion that predated deposition of the Scollard Formation, and Scollard Formation sandstone rests directly on the Wapiti Formation.

##### **4.39.2 Pick Criteria and Reference Wells**

Picks for the top of the Wapiti Formation (2 021 picks) form a subset of the wider dataset presented by Hathway (2011a), and details of data distribution, picking criteria, and type wells (00/03-04-061-23W5/0; 00/16-35-063-14W5/0) are given in that report. For cross-sections in the Edson–Whitecourt area see Hathway (2011b).

#### **4.40 Battle Formation**

The Maastrichtian Battle Formation is comprised of dark grey shales and contains tuffaceous beds such as the Kneehills Tuff (Dawson et al., 1994). It was deposited during a period of relative basin stability and low sedimentation rates (Dawson et al., 1994). Picks and descriptions for the top of the Battle Formation and base of the overlying Scollard Formation (605 picks ranging from 230 m to over 550 m subsea depth) form a subset of the wider Hathway (2011a) dataset, and further details are given in that report.

#### **4.41 Scollard Formation**

The nonmarine, Maastrichtian–Paleocene Scollard Formation consists largely of sandstone and siltstone. The upper part of the formation includes the regionally extensive Ardley coal zone (Figure 13).

##### **4.41.1 Stratigraphic Interval and Extent**

The top of the Scollard Formation is placed at the base of the first prominent thick sandstone unit above the uppermost major coal seam in the Ardley coal zone (Gibson, 1977, p. 7; see also Demchuk and Hills, 1991). In the study area, this lithostratigraphic contact, which defines the base of the overlying Paleocene Paskapoo Formation, lies at the base of laterally discontinuous fluvial channel sandstone bodies. These channel bases do not lie at a regionally consistent stratigraphic level (Figure 13; see Richardson et al., 1988, p. 10) and the surface thus defined is highly irregular.

##### **4.41.2 Pick Criteria and Reference Wells**

Information on this pick dataset can be found in Hathway (2011a) and includes picks from 8863 wells. The top of the Scollard Formation ranges in subsea depth from less than 30 m to over 350 m (Hathway, 2011a).

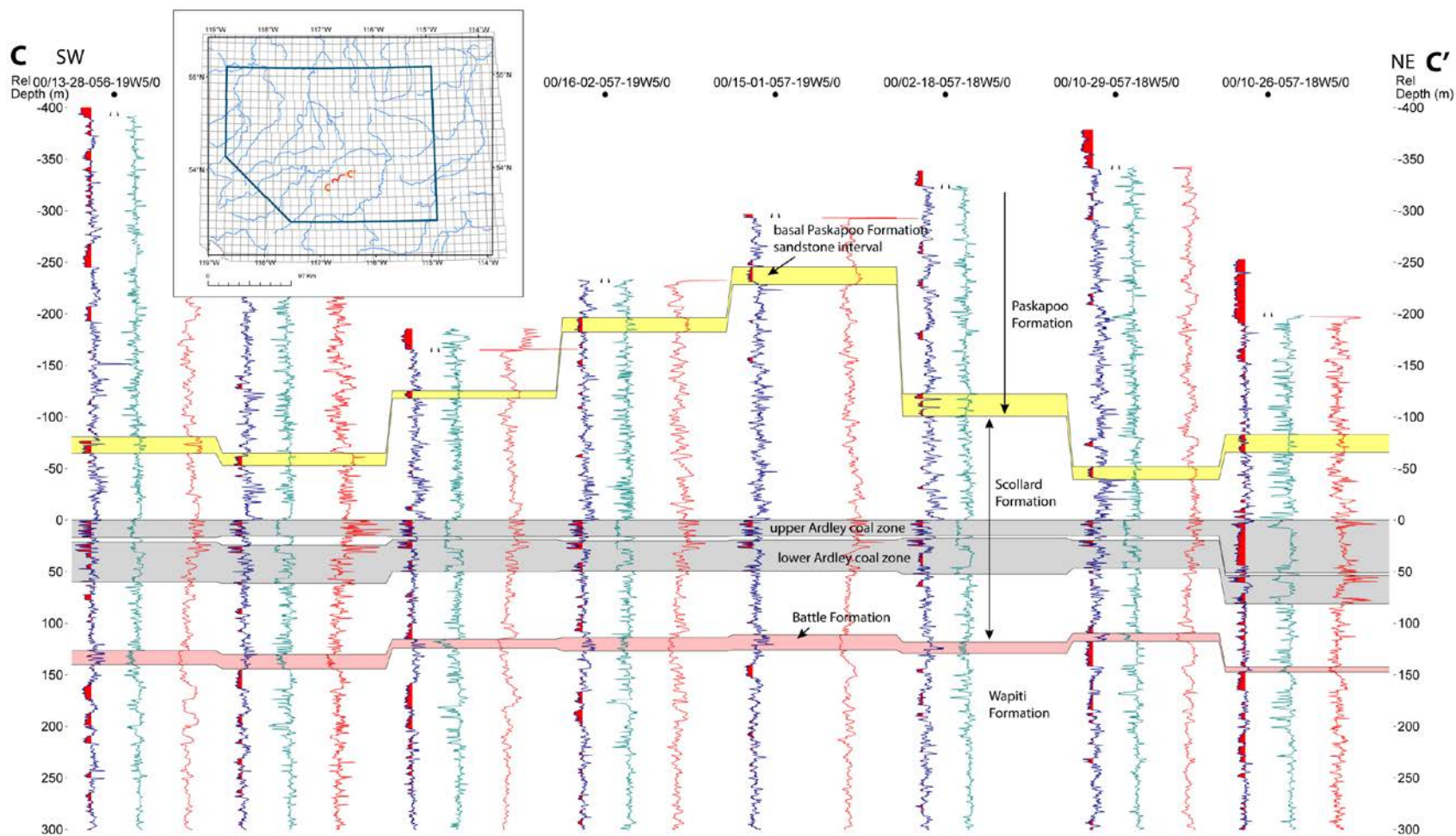


Figure 13. Stratigraphic cross-section C-C' showing lateral variability in the relative stratigraphic level of the basal Paskapoo Formation sandstone interval. Datum is the top of the Ardley coal zone in the Scollard Formation. Well logs are gamma-ray (blue line on the left, with red fill to left of 75 API cutoff), sonic (green line in the centre), and resistivity (red line on the right). Inset map shows location of cross-section (red line), west-central Alberta. Abbreviation: Rel, relative.

#### 4.42 Sub-Cretaceous Unconformity

The sub-Cretaceous unconformity is an important regional surface found throughout the study area and represents a significant period of nondeposition and erosion. Because of its regional significance, this unconformity surface has been mapped in detail (Map 573, Peterson and MacCormack, 2014). Map 573 also includes a description of the methodology for the reconstruction of sub-Cretaceous paleotopography and defining subcropping stratigraphic unit boundaries.

Initiated after the deposition of the Upper Jurassic to lowermost Cretaceous Nikanassin Formation, erosion associated with the sub-Cretaceous unconformity surface truncated Jurassic, Triassic, Permian, Mississippian, and Devonian strata, exposing the Mississippian Banff Formation within the study area. This erosive event led to highly variable topography of exposed stratigraphic units, and resulted in an intricate series of highlands and valley systems that acted as an important control on the deposition and preservation of the overlying Cretaceous succession ([Figure 6](#)).

For this study, additional sub-Cretaceous unconformity data points were incorporated into the Map 573 dataset, since the westernmost portion of the study area falls outside of the Map 573 area. In total, 2 769 data points were used to model the sub-Cretaceous unconformity surface within the study area. Subcropping unit boundaries from Map 573 were also incorporated and expanded into the study area.

### 5 Discussion: Uncertainties and Future Work

The 3D geological model of west-central Alberta contains numerous high-quality datasets of geological unit and marker horizon picks. This 3D model, as with all geological models, has some uncertainty associated with the surfaces that were generated from these picks ([Table 1](#)). Future work in the study area may help constrain regions with complex geological relationships. These relationships can be clarified in detail by examining available drillcore. Core examination of formations related to the sub-Cretaceous unconformity was conducted for this study. Additional core examination of formations, such as the Belloy, will add detail to the remaining unconformity surfaces. These additional analyses will help improve pick uncertainty, compensate for sparse data distribution, and illuminate geological complexity.

Structural offsets were noted in certain areas of the model, but these were not specifically incorporated into the model as three-dimensional planes. In the future, formational offsets and thickness changes identified in areas of high well density may be used to infer faulting. For example, deposition of the Stoddart Group is thought to have been associated with tectonic graben features of the Peace River Embayment (Barclay et al., 1990). Detailed isopachs of the Kiskatinaw and Golata formations could therefore shed light on the location of faults in the area. In addition, infill picking of formation tops around Devonian reefs could better define the edges of the reefs, whose growth patterns may have been influenced by Precambrian basement faults (Andrichuk, 1961; Edwards and Brown, 1999). Offset mapping in stratigraphic intervals with high well densities and identification of conspicuous linear geological features, including reefs, will help to identify faults and other structural features that will be incorporated into future versions of the west-central Alberta model.

There are several stratigraphic intervals that have been flagged as areas of interest for more detailed correlation and modelling. Further investigation of these items of interest will not only increase geological accuracy in the model, but will also help to reduce uncertainty in the model.

**Table 1. Calculated uncertainty for each modelled surface, including the root mean square error (RMSE).**

<b>Model Zone</b>	<b>Surface</b>	<b>Level of Uncertainty (Qualitative)</b>	<b>RMSE</b>	<b>Average Standard Error</b>	<b>Comment – Possible Cause of Uncertainty</b>
Scollard Formation	Scollard Formation top	Medium	6.5	0.01	- Lithostratigraphic boundary is not at a consistent stratigraphic level
Battle Formation	Battle Formation top	Low	4.8	0.005	- Consistent log marker
Wapiti Formation	Wapiti Formation top	Low	4.6	0.07	- Consistent log marker
Lea Park Formation / upper Puskwaskau Formation	Lea Park Formation / upper Puskwaskau Formation top	Low	1.5	0.05	- Gradational facies change
lower Puskwaskau Formation / Bad Heart Formation	Colorado Group top	Low	1.4	0.01	- Consistent log marker
upper Kaskapau Formation	Bad Heart base	Low	1.4	0.08	- Sharp contact
Muskiki Formation	Bad Heart base	Medium	1.4	0.08	- Gradational facies change
Cardium Zone Member	Cardium Zone Marker	Low	1.5	0.04	- Consistent log marker
Cardium sandstone	Cardium sandstone top	Low	1.6	0.02	- Sharp contact
Pembina River Member (excluding Cardium sandstone)	Cardium sandstone base	Medium	1.6	0.02	- Gradational facies change
Blackstone Formation / middle Kaskapau Formation	Cardium Russian Marker	Low	1.4	0.04	- Consistent log marker
Second White Specks Formation	Second White Specks Formation top	Medium	1.5	-0.05	- Minor differences in interpretation within dataset
lower Kaskapau Formation	Belle Fourche Formation top	Medium	1.7	0.05	- Minor differences in interpretation within dataset
Dunvegan Formation	Dunvegan Formation top	Medium	1.8	-0.02	- Complex, time-transgressive, lithostratigraphic boundary - not at a consistent stratigraphic level
Belle Fourche Formation / upper Shaftesbury Formation	Dunvegan Formation base	Medium	3.1	-0.02	- Complex, time-transgressive, lithostratigraphic boundary - not at a consistent stratigraphic level
Westgate Formation / lower Shaftesbury Formation	base of the Fish Scales Formation (Base of Fish Scales marker)	Low	1.4	4.7	- structural influence

<b>Model Zone</b>	<b>Surface</b>	<b>Level of Uncertainty (Qualitative)</b>	<b>RMSE</b>	<b>Average Standard Error</b>	<b>Comment – Possible Cause of Uncertainty</b>
Viking Formation / Peace River Formation (excluding Harmon Member)	Viking Formation top	Low	1.3	7.3	- stratigraphic contact with the Peace River Formation
Joli Fou Formation / Harmon Member	Joli Fou Formation top	Low	1.3	7.9	- stratigraphic contact with the Peace River Formation
Spirit River Formation / upper Mannville Group	Spirit River Formation top	Low	1.3	7.8	- structural influence
Bluesky Formation	Bluesky Formation top	Medium	1.4	7.3	- thins in areas
Gething Formation / Ostracod Beds / Ellerslie Member	Gething Formation top	Low	1.4	7.4	erosion at the base of the Gething formation in association with channel facies
Cadomin Formation	Cadomin Formation top	High	1.3	11.3	- edge of extent is complex and reliant on underlying topography - eroded by Gething channels
Nikanassin Formation	sub-Cretaceous unconformity	Low	12	10.7	- irregular erosional surface
Fernie Formation (excluding Nordegg Member)	Fernie Formation top	Low	1.3	9.5	- erosion at the sub-Cretaceous unconformity
Nordegg Member	Nordegg Member top	Low	1.3	5.3	- erosion at the sub-Cretaceous unconformity
Schooler Creek Group / Doig Formation	sub-Jurassic unconformity	Medium	1.2	5.1	- irregular erosional surface
Montney Formation	Montney Formation top	Medium	0.8	14.2	- erosional edge complex, influence of faulting
Belloy Formation	sub-Triassic unconformity	Medium	1.2	7.9	- irregular erosional surface - irregular erosional surface associated with the sub-Triassic unconformity - erosional edge complex - deposition influenced by faulting
Stoddart Group	sub-Permian unconformity	Medium	1.2	9.2	- irregular erosional surface associated with the sub-Permian unconformity - few data points
Debolt Formation	Debolt Formation top	Medium	1.4	12.5	- erosion at the sub-Triassic unconformity
Shunda Formation	Shunda Formation top	Medium	1.2	10.8	- erosion at the sub-Jurassic and sub-Cretaceous unconformities

Model Zone	Surface	Level of Uncertainty (Qualitative)	RMSE	Average Standard Error	Comment – Possible Cause of Uncertainty
Pekisko Formation	Pekisko Formation top	Low	1.2	9.3	- erosion at the sub-Cretaceous unconformity
Banff Formation	Banff Formation top	Low	1.2	9.1	- patchy data in SW
Exshaw Formation	Exshaw Formation top	Low	1.2	9.9	- data missing in SW, patchy in SE
Wabamun Group	Wabamun Group top	Low	1.2	9.6	- data missing in SW
Graminia Silt Member	Graminia Silt Member top	Low	1.2	11.7	- draping on Blueridge Member reefs influences z value
Blue Ridge Member	Blue Ridge Member top	Low	1.1	11.9	- Blueridge contains reefs
Calmar Formation	Calmar Formation top	Medium	1.2	13.4	- draping on Leduc reefs influences z value
Nisku Formation	Nisku Formation top	Medium	1.2	13.7	- draping on Leduc reefs influences z value
Ireton Formation (above Ireton Z marker)	Ireton Formation top	Medium	1.3	10.2	- clustered data due to presence of Leduc reefs
Ireton Formation (below Ireton Z marker)	Ireton Z Marker top	Low	1.4	8.4	- clustered data due to presence of Leduc reefs
Duvernay Formation	Duvernay Formation top	Low	1.4	7.1	- clustered data due to presence of Leduc reefs
Leduc Formation	Leduc Formation top	Medium			- sparse data in some areas
Majeau Lake Formation	Majeau Lake Formation top	Low	1.2	5.4	- clustered data due to presence of Leduc reefs
Waterways Formation	Waterways Formation top	High	1.4	8.4	- patchy data in SW
Swan Hills Formation / Slave Point Formation	Swan Hills Formation	High	2.22	-0.06	- some uncertainty in pick dataset
	Slave Point Formation	High	1.50	0.6	- some uncertainty in pick dataset
Watt Mountain Formation to Precambrian interval	Watt Mountain Formation top	High	1.3	6.5	- patchy data in SW

## 5.1 Paleozoic Intervals for Investigation

- Outlines of Devonian reef, platform, or bank edges could be updated in future versions of the model with infill picks in wells along these boundaries.
- The nature of the Woodbend Group shales (Majeau Lake, Duvernay, and Ireton formations) changes drastically toward the eastern portion of the study area. A breakdown of the internal stratigraphy of the Ireton and Duvernay clinofolds would aid in correlation of depositional cycles and help to determine where the uppermost cycle of the Grosmont Formation is present within the upper Woodbend Group shales.
- Outlines of Zeta Lake Member reefs and other buildups within the Nisku Formation have not been created or incorporated into this version of the model. The paleogeography of this area during Nisku Formation deposition is highly complex, as many small sub-basins existed near the end of this long reef-building cycle during the Middle to Late Devonian. Correlating members within the Nisku

Formation would aid in defining reef edges, sub-basin boundaries, and would also provide more insight into the transition from Woodbend Group to Winterburn Group shale deposition.

- Units within the Elk Point Group and Cambrian stratigraphy were not individually modelled in this version of the model. In much of the study area, a lack of good well control made it difficult to accurately identify these units at the same resolution as other stratigraphic intervals. In the future, if additional well control becomes available, these units could be incorporated in the model.

## 5.2 Mesozoic Intervals for Investigation

- The influence of the sub-Triassic unconformity on the deposition of the Montney Formation needs to be further explored through detailed isopach mapping. Unconformities within the Upper Triassic (such as the Coplin unconformity) could be mapped. The edge of the Nordegg Member carbonate platform in the southeast could be mapped to differentiate the Nordegg Member from the highly radioactive Gordondale Member. Additionally, the sub-Jurassic unconformity (the base of the Nordegg Member) could be mapped in detail, as done with the sub-Cretaceous unconformity.
- The internal stratigraphy of the upper Fernie Formation could be differentiated in more detail, such as mapping the extent of the Rock Creek Member. The regional unconformity separating the Upper Jurassic deposits from the underlying units (Poulton et al., 1994) could be evaluated. Additionally, the relationship between upper Fernie Formation deposition and the underlying topography associated with this unconformity could be examined in more detail.
- The internal stratigraphy of the upper Nikanassin Formation is not well defined and is difficult to pick out on well logs (Poulton et al., 1990). Additional core work would help differentiate the internal stratigraphy. Once enough picks have been made to define this interval, it could be modelled and incorporated within the regional model.
- The top of the Cadomin Formation / base of the Gething Formation could be mapped at a higher well density to better ascertain the unconformity surface. The onlapping relationship with the Fox Creek Escarpment also could be better defined to differentiate between the Cadomin Formation and basal Gething Formation channels along the escarpment.
- The lateral transition of the Gething Formation into the Ellerslie Member and Ostracod Beds could be differentiated and mapped for incorporation into the model. Because this transition occurs within the southeastern corner of the study area, the top of the Ostracod Beds was mapped as the top of the Gething Formation. This example highlights a specific regional stratigraphic challenge, namely, mapping units across stratigraphic nomenclature boundaries. These boundaries mark transitions between time-equivalent, but lithologically distinct units. The transition between units is complex, often involving interfingering or erosion, and therefore a detailed approach is required.
- To add stratigraphic detail, the internal members of the Spirit River Formation could be differentiated and mapped. The transition of the Spirit River Formation to the upper Mannville Group could also be investigated in detail so as to illustrate nomenclature boundaries within the model region. Additionally, core studies could be done to confirm the well log derived data.
- Further regional nomenclature transitions, such as the lateral transition from the Joli Fou Formation to the lower Paddy Member of the Peace River Formation (equivalent to the Joli Fou Formation) and that of the Viking Formation to the Paddy Member of the Peace River Formation, could be examined in detail. Characterization of this transition could be improved through additional analysis, such as core examination, and would also help better define the Albian–Cenomanian boundary.
- Lastly, some zero edges generated by the model were not in complete agreement with those generated by the stratigrapher. This issue was most notable with the Cadomin Formation, and could be resolved by picking the formation in additional wells, which would help delineate a more accurate geoeage.

## 5.3 Modelling Complications

During model construction, some issues arose regarding geologically inaccurate representations of data by Petrel. Specifically, the Duvernay Formation and Ireton Formation surfaces in the model appear to

climb the sides of the Leduc Formation reefs when the model is shown with high vertical exaggeration (Figure 4). The volumetric impact of this ‘draping effect’ is negligible. This is merely a visual effect, as the model was built with an orthogonal grid of 500 m × 500 m grid cells oriented in the same direction. This caused a draping effect on the sides of the reefs, in areas where a data point was located near the edge of a grid cell in data-poor regions. Future versions of the model will address this issue by using a smaller grid-cell size (surfaces produced using ArcMap will be imported directly into Petrel). Surface artifacts were also observed within data-poor regions in the corner of the model (displayed in Figure 4). These artifacts appear as sharp linear features on the modelled surface in Petrel. Likewise, data-rich regions were artifact free (regardless of which program was used for modelling). Future versions of this model could minimize these artifacts by increasing data density.

## 6 Summary

Building a 3D geological model of west-central Alberta was undertaken as part of the larger goal to map the entire province as part of the Geological Framework Project. The model contains 49 geological surfaces from the top of the Precambrian to the top of bedrock.

Overall, the 3D geological model of west-central Alberta provides a framework of geologically important horizons and crucial information on how these surfaces relate to one another in 3D space. The 3D visualization allows for new insights into complex stratigraphic relationships, and a look at the paleotopography that existed throughout geological time in west-central Alberta. This report is intended to support the 3D model and the data that were used to create the model, address any discrepancies associated with crossing lateral stratigraphic nomenclature boundaries, and also explain the inclusion or exclusion of certain geological features in the study area.

## 7 References

- Aitken, J.D. (1968): Cambrian sections in the easternmost southern Rocky Mountains and the adjacent subsurface, Alberta; Geological Survey of Canada, Paper 66–23, 96 p.
- Alberta Geological Survey (2015): Alberta Table of Formations; Alberta Energy Regulator; URL <<https://ags.aer.ca/activities/table-of-formation>> [November 2018].
- Andrichuk, J.M. (1961): Stratigraphic evidence for tectonic and current control of Upper Devonian reef sedimentation Duhamel area, Alberta, Canada; American Association of Petroleum Geologists Bulletin, v. 45, p. 612–632.
- Armitage, I.A., Pemberton, S.G. and Moslow, T.F. (2004): Facies succession, stratigraphic occurrence, and paleogeographic context of conglomeratic shorelines within the Falher “C”, Spirit River Formation, Deep Basin, west central Alberta; Bulletin of Canadian Petroleum Geology, v. 52, p. 39–56.
- Atchley, S.C., James, S.C., Harlow, H., Leslie, C., Jiang, J., Carrelli, G., Bindon, W. and Beal, J. (2018): Geological and resource assessment of the Upper Devonian Grosmont and upper Ireton Formations, central Grosmont shelf complex, Alberta, Canada. American Association of Petroleum Geologists Bulletin, v. 102, p. 731–759.
- Barclay, J.E. (1989): Evolution of a Carboniferous, incised shelf sequence – Golata Formation, western Canada; Geological Survey of Canada, Open File 2030, 1 p.
- Barclay, J.E. and Davies, G.R. (1989): Tidal deposits – Carboniferous Kiskatinaw Formation, Alberta and a modern analogue – Shark Bay, western Australia; *in* Modern and ancient examples of clastic tidal deposits – a core and peel workshop, G.E. Reinson (ed.), Canadian Society of Petroleum Geologists and Society of Economic Paleontologists and Mineralogists, Calgary, Alberta, p. 117–126.
- Barclay, J.E., Krause, F.F., Campbell, R.I. and Utting, J. (1990): Dynamic casting and growth faulting: Dawson Creek Graben Complex, Carboniferous-Permian Peace River embayment, western Canada; Bulletin of Canadian Petroleum Geology, v. 38A, p. 115–145.
- Bhattacharya, J.P. (1994): Cretaceous Dunvegan Formation strata of the Western Canada Sedimentary Basin; *in* Geological atlas of the Western Canada Sedimentary Basin, G.D. Mossop and I. Shetsen (comp.), Canadian Society of Petroleum Geologists and Alberta Research Council, p. 365–373.
- Bloch, J., Schroder-Adams, C., Leckie, D.A., McIntyre, D.J., Craig, J. and Staniland, M. (1993): Revised stratigraphy of the lower Colorado Group (Albian to Turonian), western Canada; Bulletin of Canadian Petroleum Geology, v. 41, p. 325–348.
- Branscombe, P., MacCormack, K.E., Corlett, H., Hathway, B., Hauck, T.E. and Peterson, J.T. (2018): 3D Provincial Geological Framework Model of Alberta, Version 1 (dataset, multiple files); Alberta Energy Regulator, AER/AGS Model 2017-03, URL <[https://ags.aer.ca/data-maps-models/3D\\_PGF\\_model\\_v1.html](https://ags.aer.ca/data-maps-models/3D_PGF_model_v1.html)> [June 2018].
- Cant, D.J. (1984): Development of shoreline-shelf sand bodies in a Cretaceous epeiric sea deposit; Journal of Sedimentary Petrology, v. 54, p. 541–556.
- Cant, D.J. and Abrahamson, B. (1996): Regional distribution and internal stratigraphy of the Lower Mannville; Bulletin of Canadian Petroleum Geology, v. 44, p. 508–529.
- Casas, J.E. and Walker, R.G. (1997): Sedimentology and depositional history of Units C and D of the Falher Member, Spirit River Formation, west central Alberta; Bulletin of Canadian Petroleum Geology, v. 45, p. 218–238.

- Chalmers, G.R.L. and Bustin, R.M. (2012): Geological evaluation of Halfway-Doig-Montney hybrid gas shale – tight gas reservoir, northeastern British Columbia; *Marine and Petroleum Geology*, v. 38, p. 53–72.
- Dafoe, L.T., Gingras, M.K. and Pemberton, S.G. (2010): Wave-influenced deltaic sandstone bodies and offshore deposits in the Viking Formation, Hamilton Lake area, south-central Alberta, Canada; *Bulletin of Canadian Petroleum Geology*, v. 58, p. 173–201.
- Davies, G.R. (1997): The Triassic of the Western Canada Sedimentary Basin: tectonic and stratigraphic framework, Palaeogeography, Paleoclimate and biota; *in* Triassic of the Western Canada Sedimentary Basin, T.F. Moslow and J. Wittenberg (ed.), *Bulletin of Canadian Petroleum Geology*, v. 45, p. 434–460.
- Dawson, F.M., Evans, C.G., Marsh, R. and Richardson, R. (1994): Uppermost Cretaceous and Tertiary strata of the Western Canada Sedimentary Basin; *in* Geological atlas of the Western Canada Sedimentary Basin, G.D. Mossop and I. Shetsen (comp.), Canadian Society of Petroleum Geologists and Alberta Research Council, p. 387–406, URL <<https://ags.aer.ca/publications/chapter-24-uppermost-cretaceous-and-tertiary-strata.htm>> [April 2019].
- Demchuk, T.D. and Hills, L.V. (1991): A re-examination of the Paskapoo Formation in the central Alberta Plains: the designation of three new members; *Bulletin of Canadian Petroleum Geology*, v. 39, no. 3, p. 270–282.
- Deutsch, C.V. and Journel, A.G. (1992): *Geostatistical Software Library and User's Guide*; Oxford University Press, 340 p.
- Dunn, L.A., Schmidt, G., Hammermaster, K., Brown, M., Bernard, R., Wen, E., Befus, R. and Gardiner, S. (2012): The Duvernay Formation (Devonian): sedimentology and reservoir characterization of a shale gas/liquids play in Alberta, Canada; Canadian Society of Petroleum Geologists, Annual Core Convention program with abstracts, May 14–18, 2012, Calgary, Alberta.
- Edwards, D. and Brown, R.J. (1999): Understanding the influence of Precambrian crystalline basement on Upper Devonian carbonates in central Alberta from a geophysical perspective; *Bulletin of Canadian Petroleum Geology*, v. 47, p. 412–438.
- Edwards, D.E., Barclay, J.E., Gibson, D.W., Kville, G.E. and Halton, E. (1994): Triassic strata of the Western Canada Sedimentary Basin; *in* Geological atlas of the Western Canada Sedimentary Basin, G.D. Mossop and I. Shetsen (comp.), Canadian Society of Petroleum Geologists and Alberta Research Council, p. 259–275, URL <<https://ags.aer.ca/publications/chapter-16-triassic-strata.htm>> [April 2019].
- Fanti, F. and Catuneanu, O. (2009): Stratigraphy of the Upper Cretaceous Wapiti Formation, west central Alberta, Canada; *Canadian Journal of Earth Sciences*, v. 46, no. 4, p. 263–286.
- Fenton, M.M., Schreiner, B.T., Nielsen, E. and Pawlowicz, J.G. (1994): Quaternary geology of the Western Plains; *in* Geological atlas of the Western Canada Sedimentary Basin, G.D. Mossop and I. Shetsen (comp.), Canadian Society of Petroleum Geologists and Alberta Research Council, p. 413–420, URL <<https://ags.aer.ca/publications/chapter-26-quaternary-geology-of-the-western-plains>> [April 2019].
- Geldsetzer, H.H. (1988): Ancient Wall reef complex, Frasnian age, Alberta; *in* Reefs, Canada and adjacent areas, H.H. Geldsetzer, N.P. James and G.E. Tebbut (ed.), Canadian Society of Petroleum Geologists, Memoir 13, p. 431–439.
- Gibson, D.W. (1977): Upper Cretaceous and Tertiary coal-bearing strata in the Drumheller-Ardley region, Red Deer River valley, Alberta; Geological Survey of Canada, Paper 76–35, 41 p.

- Gingras, M.K., Zonneveld, J.P. and Blakney, B.J. (2010): Preliminary assessment of ichnofacies in the Gething Formation of NE British Columbia; *Bulletin of Canadian Petroleum Geology*, v. 58, p. 159–172.
- Glass, D.J. (1990): *Lexicon of Canadian stratigraphy, volume 4: western Canada*; Canadian Society of Petroleum Geologists, Calgary, Alberta.
- Glombick, P.M. (2013): Subsurface stratigraphic picks for the base of the Belly River Group/Wapiti Formation, Alberta Plains (tabular data, tab delimited format); Energy Resources Conservation Board, ERCB/AGS Digital Data 2013-0029.
- Green, D.G. and Mountjoy, E.W. (2005): Fault and conduit controlled burial dolomitization of the Devonian west central Alberta Deep Basin; *Bulletin of Canadian Petroleum Geology*, v. 53, p. 101–129.
- Halbertsma, H.L. (1959): Nomenclature of Upper Carboniferous and Permian strata in the subsurface of the Peace River area; *Journal of Alberta Society of Petroleum Geologists*, v. 7, p. 109–118.
- Halbertsma, H.L. (1994): Devonian Wabamun Group of the Western Canada Sedimentary Basin; *in Geological atlas of the Western Canada Sedimentary Basin*, G.D. Mossop and I. Shetsen, (comp.), Canadian Society of Petroleum Geologists and Alberta Research Council, p. 203–220.
- Hathway, B. (2011a): Tops of the Horseshoe Canyon, Wapiti and Battle formations in the west central Alberta Plains: subsurface stratigraphic picks and modelled surface; Energy Resources Conservation Board, ERCB/AGS Open File 2011-08, 24 p.
- Hathway, B. (2011b): Late Maastrichtian paleovalley systems in west central Alberta: mapping the Battle Formation in the subsurface; *Bulletin of Canadian Petroleum Geology*, v. 59, no. 3, p. 195–206.
- Hauck, T.E. (2014): Regional correlation of the Beaverhill Lake Group in the subsurface of Alberta Townships 29 to 113 and Ranges 1W4 to 13W6; Alberta Energy Regulator, AER/AGS Open File 2014-05, 29 p.
- Hayes, B.J.R., Christopher, J.E., Rosenthal, L., McKercher, B., Minken, D., Tremblay, Y.M. and Fennell, J. (1994): Cretaceous Mannville Group of the Western Canada Sedimentary Basin; *in Geological atlas of the Western Canada Sedimentary Basin*, G.D. Mossop and I. Shetsen (comp.), Canadian Society of Petroleum Geologists and Alberta Research Council, p. 317–334, URL <<https://ags.aer.ca/publications/chapter-19-cretaceous-mannville-group>> [April 2019].
- Henderson, C.M., Richards, B.C. and Barclay, J.E. (1994): Permian strata of the Western Canada Sedimentary Basin; *in Geological atlas of the Western Canada Sedimentary Basin*, G.D. Mossop and I. Shetsen (comp.), Canadian Society of Petroleum Geologists and Alberta Research Council, p. 251–258, URL <<https://ags.aer.ca/publications/chapter-15-permian-strata>> [April 2019].
- Hu, Y.G. and Plint, A.G. (2009): An allostratigraphic correlation of a mudstone-dominated, syn-tectonic wedge: the Puskwaskau Formation (Santonian-Campanian) in outcrop and subsurface, Western Canada Foreland Basin; *Bulletin of Canadian Petroleum Geology*, v. 57, no. 1, p. 1–33.
- Hubbard, S.M., Gingras, M.K. and Pemberton, S.G. (2004): Palaeoenvironmental implications of trace fossils in estuarine deposits of the Cretaceous Bluesky Formation, Cadotte region, Alberta, Canada; *in Trace fossils in evolutionary palaeoecology*, B.D. Webby, M.G. Mángano and L.A. Buatois (ed.), *Fossils and Strata*, v. 51, p. 1–20.
- Hubbard, S.M., Gingras, M.K., Pemberton, S.G. and Thomas, M.B. (2002): Variability in wave-dominated estuary sandstones: implications on subsurface reservoir development; *Bulletin of Canadian Petroleum Geology*, v. 50, p. 118–137.
- Journel, A.G. and Huijbregts, C.J., (1978): *Mining geostatistics*; Academic Press, London, 600 p.

- Kramers, J.W. and Lerbekmo, J.K. (1967): Petrology and mineralogy of Watt Mountain Formation, Mitsue-Nippisi area, Alberta; *Bulletin of Canadian Petroleum Geology*, v. 15, p. 346–378.
- Krause, F.F. and Nelson, D.A. (1984): Storm event sedimentation: lithofacies association in the Cardium Formation, Pembina area, west central Alberta, Canada; *in* *The Mesozoic of middle North America*, D.F. Stott and D.J. Glass (ed.), Canadian Society of Petroleum Geologists, Memoir 9, p. 485–511.
- Krause, F.F., Deutsch, K.B., Joiner, S.D., Barclay, J.E., Hall, R.L. and Hills, L.V. (1994): Cretaceous Cardium Formation of the Western Canada Sedimentary Basin; *in* *Geological atlas of the Western Canada Sedimentary Basin*, G.D. Mossop and I. Shetsen (comp.), Canadian Society of Petroleum Geologists and Alberta Research Council, p. 374–385.
- Law, J. (1981): Mississippian correlations, northeastern British Columbia, and implications for oil and gas exploration; *Bulletin of Canadian Petroleum Geology*, v. 29, p. 378–398.
- Leckie, D.A. and Cheel, R.J. (1997): Sedimentological and depositional history of Lower Cretaceous coarse-grained clastics, southwest Alberta and southeast British Columbia; *Bulletin of Canadian Petroleum Geology*, v. 45, p. 1–24.
- Leckie, D.A., Schröder-Adams, C.J., Rosenthal, L. and Wall, J.H. (2000): An outcrop of Albian Viking Formation and a southerly extension of the Hulcross/Harmon interval in west central Alberta; *Bulletin of Canadian Petroleum Geology*, v. 48, p. 30–42.
- Macauley, G. (1958): Late Paleozoic of Peace River area, Alberta; *in* *Jurassic and Carboniferous of western Canada*, A.J. Goodman (ed.), American Association of Petroleum Geologists, p. 289–308.
- Mackay, D.A. and Dalrymple, R.W. (2011): Dynamic mud deposition in a tidal environment: the record of fluid-mud deposition in the Cretaceous Bluesky Formation, Alberta, Canada; *Journal of Sedimentary Research*, v. 81, p. 901–920.
- Macqueen, R.W. and Sandberg, C.A. (1970): Stratigraphy, age and interregional correlation of the Exshaw Formation, Alberta Rocky Mountains; *Bulletin of Canadian Petroleum Geology*, v. 18, no. 1, p. 32–66.
- McLean, R.A. and Klapper, G. (1998): Biostratigraphy of Frasnian (Upper Devonian) strata in western Canada, based on conodonts and rugose corals; *Bulletin of Canadian Petroleum Geology*, v. 46, p. 515–563.
- Meijer Drees, N.C. (1994): Devonian Elk Point Group of the Western Canada Sedimentary Basin; *in* *Geological atlas of the Western Canada Sedimentary Basin*, G.D. Mossop and I. Shetsen (comp.), Canadian Society of Petroleum Geologists and Alberta Research Council, p. 129–147, URL <<https://ags.aer.ca/publications/chapter-10-devonian-elk-point-group.htm>> [April 2019].
- Meijer Drees, N.C. and Johnston, D.I. (1993): Geology of the Devonian-Carboniferous boundary beds in Alberta; Canadian Society of Petroleum Geologists Special Publications, Carboniferous to Jurassic: Pangea: Core workshop guidebook, p. 188–205.
- Meijer Drees, N.C., Johnston, D.I. and Fowler, M.G. (1998): Lithology, biostratigraphy and geochemistry of the Upper Devonian Graminia Formation, central Alberta; *Bulletin of Canadian Petroleum Geology*, v. 46, p. 148–165.
- Naqvi, I.H. (1972): The Belloy Formation (Permian), Peace River area, northern Alberta and northeastern British Columbia; *Bulletin of Canadian Petroleum Geology*, v. 20, p. 58–88.
- O’Connell, S.C. (1988): The distribution of Bluesky facies in the region overlying the Peace River arch, northwestern Alberta; *in* *Sequences, stratigraphy, sedimentology: surfaces and subsurface*, D.P. James and D.A. Leckie (ed.), Canadian Society of Petroleum Geologists, Memoir 15, p. 387–400.

- O'Connell, S.C. (1990): The development of the Lower Carboniferous Peace River embayment as determined from Banff and Pekisko formation depositional patterns; *Bulletin of Canadian Petroleum Geology*, v. 38A, p. 93–114.
- Oldale, R.S. and Munday, R.J. (1994): Devonian Beaverhill Lake Group of the Western Canada Sedimentary Basin; *in Geological atlas of the Western Canada Sedimentary Basin*, G.D. Mossop and I. Shetsen (comp.), Canadian Society of Petroleum Geologists and Alberta Research Council, p. 149–163.
- Peterson, J.T. and MacCormack, K.E. (2014): Paleotopography of the sub-Cretaceous unconformity surface, west-central Alberta; Alberta Energy Regulator, AER/AGS Map 573, URL <[https://ags.aer.ca/publications/MAP\\_573.html](https://ags.aer.ca/publications/MAP_573.html)> [April 2019].
- Plint, A.G. (1990): An allostratigraphic correlation of the Muskiki and Marshybank formations (Coniacian-Santonian) in the Foothills and subsurface of the Alberta Basin; *Bulletin of Canadian Petroleum Geology*, v. 38, no. 3, p. 288–306.
- Plint, A.G. (2000): Sequence stratigraphy and paleogeography of a Cenomanian deltaic complex: the Dunvegan and lower Kaskapau formations in subsurface and outcrop, Alberta and British Columbia, Canada; *Bulletin of Canadian Petroleum Geology*, v. 48, p. 43–79.
- Plint, A.G., Norris, B. and Donaldson, S. (1990): Revised definitions for the Upper Cretaceous Bad Heart Formation and associated units in the Foothills and Plains of Alberta and British Columbia; *Bulletin of Canadian Petroleum Geology*, v. 38, no. 1, p. 78–88.
- Poulton, T.P., Tittlemore, J. and Dolby, G. (1990): Jurassic strata of northwestern (and west central) Alberta and northeastern British Columbia; *Bulletin of Canadian Petroleum Geology*, v. 38A, p. 159–175.
- Poulton, T.P., Christopher, J.E., Hayes, B.J.R., Losert, J., Tittlemore, J. and Gilchrist, R.D. (1994): Jurassic and lowermost Cretaceous strata of the Western Canada Sedimentary Basin; *in Geological atlas of the Western Canada Sedimentary Basin*, G.D. Mossop and I. Shetsen (comp.), Canadian Society of Petroleum Geologists and Alberta Research Council, p. 297–316, URL <<https://ags.aer.ca/publications/chapter-18-jurassic-and-lowermost-cretaceous-strata.htm>> [April 2019].
- Putnam, P.E. and Ward, G.S. (2001): The relation between stratigraphic elements, pressure regime, and hydrocarbons in the Alberta deep basin (with emphasis on select Mesozoic units); *American Association of Petroleum Geologists Bulletin*, v. 85, p. 691–714.
- Reinson, G.E., Warters, W.J., Cox, J. and Price, P.R. (1994): Cretaceous Viking Formation of the Western Canada Sedimentary Basin; *in Geological atlas of the Western Canada Sedimentary Basin*, G.D. Mossop and I. Shetsen (comp.), Canadian Society of Petroleum Geologists and Alberta Research Council, p. 353–363, URL <<https://ags.aer.ca/publications/chapter-21-cretaceous-viking-formation>> [April 2015].
- Richards, B.C. (1989): Upper Kaskaskia sequence: uppermost Devonian and Lower Carboniferous; *in Western Canada Sedimentary Basin – a case history*, B.D. Ricketts (ed.), Canadian Society of Petroleum Geologists, Special Publication no. 30, p. 165–201.
- Richards, B.C., Barclay, J.E., Bryan, D., Hartling, A., Henderson, C.M. and Hinds, R.C. (1994): Carboniferous strata of the Western Canada Sedimentary Basin; *in Geological atlas of the Western Canada Sedimentary Basin*, G.D. Mossop and I. Shetsen (comp.), Canadian Society of Petroleum Geologists and Alberta Research Council, p. 221–250, URL <<https://ags.aer.ca/publications/chapter-18-jurassic-and-lowermost-cretaceous-strata>> [April 2019].

- Richardson, R.J.H., Strobl, R.S., MacDonald, D.E., Nurkowski, J.R., McCabe, E.J. and Bosman, A. (1988): An evaluation of coal resources of the Ardley coal zone to a depth of 400 m in the Alberta Plains area; Alberta Research Council, ARC/AGS Open File Report 1988-02, 85 p.
- Riediger, C.L. (2002): Hydrocarbon source rock potential and comments on correlation of the Lower Jurassic Poker Chip shale, west central Alberta; *Bulletin of Canadian Petroleum Geology*, v. 50, p. 263–276.
- Riediger, C.L., Fowler, M.G., Snowdon, L.R., Goodarzi, F. and Brooks, P.W. (1990): Source rock analysis of the Lower Jurassic “Nordegg Member” and oil-source rock correlations, northwestern Alberta and northeastern British Columbia; *Bulletin of Canadian Petroleum Geology*, v. 38A, p. 236–249.
- Rottenfusser, B.A. and Oliver, T.A. (1977): Depositional environments and petrology of the Gilwood Member north of the Peace River Arch; *Bulletin of Canadian Petroleum Geology*, v. 25, p. 907–928.
- Slind, O.L., Andrews, G.D., Murray, D.L., Norford, B.S., Paterson, D.F., Salas, C.J. and Tawadros, E.E. (1994): Middle Cambrian to Lower Ordovician strata of the Western Canada Sedimentary Basin; *in Geological atlas of the Western Canada Sedimentary Basin*, G.D. Mossop and I. Shetsen (comp.), Canadian Society of Petroleum Geology and Alberta Research Council, p. 87–108.
- Smith, D.G., Zorn, C.E. and Sneider, R.M. (1984): The paleogeography of the Lower Cretaceous of western Alberta and northeastern British Columbia in and adjacent to the deep basin of the Elmworth area; *in Elmworth – case study of a deep basin gas field*, J.A. Masters (ed.), American Association of Petroleum Geologists, Memoir 38, p. 79–114.
- Smith, M.G. and Bustin, R.M. (2000): Late Devonian and Early Mississippian Bakken and Exshaw black shale source rocks, Western Canada Sedimentary Basin: a sequence stratigraphic interpretation; *American Association of Petroleum Geologists, Bulletin*, v. 84, p. 940–960.
- Stoakes, F.A. (1980): Nature and control of shale basin-fill and its effects on reef growth and termination: Upper Devonian Duvernay and Ireton formations of Alberta, Canada; *Bulletin of Canadian Petroleum Geology*, v. 28, p. 345–410.
- Stoakes, F.A. (1992a): Winterburn megasequence; *in Devonian-Early Mississippian carbonates of the Western Canada Sedimentary Basin: a sequence stratigraphic framework*, J.C. Wendte, F.A. Stoakes and C.V. Campbell (ed.), Society of Economic Paleontologists and Mineralogists, Short Course No. 28, June 20–21, 1992, Calgary, Alberta, p. 207–224.
- Stoakes, F.A. (1992b): Woodbend megasequence; *in Devonian-Early Mississippian carbonates of the Western Canada Sedimentary Basin: a sequence stratigraphic framework*, J.C. Wendte, F.A. Stoakes and C.V. Campbell (ed.), Society of Economic Paleontologists and Mineralogists, Short Course No. 28, June 20–21, 1992, Calgary, Alberta, p. 183–206.
- Stoakes, F.A. (1992c): Wabamun megasequence; *in Devonian-Early Mississippian carbonates of the Western Canada Sedimentary Basin: a sequence stratigraphic framework*, J.C. Wendte, F.A. Stoakes and C.V. Campbell (ed.), Society of Economic Paleontologists and Mineralogists, Short Course No. 28, June 20–21, 1992, Calgary, Alberta, p. 225–239.
- Stoakes, F.A. and Creaney, S. (1984): Sedimentology of a carbonate source rock: Duvernay Formation of central Alberta; *in Carbonates in subsurface and outcrop*, L. Eliuk (ed.), Proceedings of the 1984 Canadian Society of Petroleum Geologists Core Conference, Calgary, Alberta, p. 132–147.
- Stoakes, F.A. and Wendte, J.C. (1987): The Woodbend Group; *in Devonian lithofacies and reservoir styles in Alberta*, F.F. Krause and O.G. Burrowes (ed.), 13th Canadian Society of Petroleum Geologists Core Conference and Display, Aug. 19–21, 1987, Calgary, Alberta, p. 153–170.

- Stott, D.F. (1963): The Cretaceous Alberta Group and equivalent rocks, Rocky Mountain Foothills, Alberta and British Columbia; Geological Survey of Canada, Memoir 317, 306 p.
- Stott, D.F. (1967): The Cretaceous Smoky Group, Rocky Mountain Foothills, Alberta and British Columbia; Geological Survey of Canada, Bulletin 132, 133 p.
- Switzer, S.B., Holland, W.G., Christie, D.S., Graf, G.C., Hedinger, A., McAuley, R., Wierzbicki, R. and Packard, J.J. (1994): Devonian Woodbend-Winterburn strata of the Western Canada Sedimentary Basin; *in* Geological atlas of the Western Canada Sedimentary Basin, G.D. Mossop and I. Shetsen (comp.), Canadian Society of Petroleum Geologists and Alberta Research Council, p. 165–202.
- Tu, Q., Schröder-Adams, C.J. and Craig, J. (2007): A new lithostratigraphic framework for the Cretaceous Colorado Group in the Cold Lake heavy oil area, east-central Alberta, Canada; *Natural Resources Research*, v. 16, no. 1, p. 17–30.
- Varban, B.L. and Plint, A.G. (2005): Allostratigraphy of the Kaskapau Formation (Cenomanian-Turonian) in subsurface and outcrop: NE British Columbia and NW Alberta, Western Canada Foreland Basin; *Bulletin of Canadian Petroleum Geology*, v. 53, p. 357–389.
- Wadsworth, J., Blyd, R., Diessel, C., Leckie, D. and Zaitlin, B.A. (2002): Stratigraphic style of coal and non-marine strata in a tectonically influenced intermediate accommodation setting: the Mannville Group of the Western Canadian Sedimentary Basin, south-central Alberta; *Bulletin of Canadian Petroleum Geology*, v. 50, p. 507–541.
- Watts, N.R. (1987): Carbonate sedimentology and depositional history of the Nisku Formation in south-central Alberta; *in* Devonian lithofacies and reservoir styles in Alberta, F.F. Krause and O.G. Burrowes (ed.), 13th Canadian Society of Petroleum Geologists Core Conference and Display, Aug. 19–21, 1987, Calgary, Alberta, p. 87–152.
- Webb, A.C., Schröder-Adams, C.J. and Pedersen, P.K. (2005): Regional subsurface correlations of Albian sequences north of the Peace River in NE British Columbia: northward extent of sandstones of the Falher and Notikewin members along the eastern flank of the foredeep; *Bulletin of Canadian Petroleum Geology*, v. 53, p. 165–188.
- Wendte, J.C. (1992): Evolution of the Judy Creek Complex, a late Middle Devonian isolate platform-reef complex in west-central Alberta; *in* Devonian-Early Mississippian carbonates of the Western Canada Sedimentary Basin: a sequence stratigraphic framework, J. Wendte, F. A. Stoakes, C. V. Campbell (ed.), Society of Economic Paleontologists and Mineralogists, Short Course No. 28, June 20–21, 1992, Calgary, Alberta, p. 89-125.
- Wendte, J.C. (1998): Devonian summary cross-section, Wild River basin, west-central Alberta; Geological Survey of Canada, Open File No. 3677, 2 sheets, URL <<https://geoscan.nrcan.gc.ca/starweb/geoscan/servlet.starweb?path=geoscan/download.web&search1=R=210022>> [June 2016].
- Wendte, J.C. and Uyeno, T. (2005): Sequence stratigraphy and evolution of Middle to Upper Devonian Beaverhill Lake strata, south-central Alberta; *Bulletin of Canadian Petroleum Geology*, v. 53, p. 250–354.
- Wendte, J.C., Stoakes, F.A., Bosman, M. and Bernstein, L. (1995): Genetic and stratigraphic significance of the Upper Devonian Frasnian Z Marker, west-central Alberta; *Bulletin of Canadian Petroleum Geology*, v. 43, p. 339–406.
- White, J.M. and Leckie, D.A. (1999): Palynological age constraints on the Cadomin and Dalhousie formations in SW Alberta; *Bulletin of Canadian Petroleum Geology*, v. 47, p. 199–222.

- Williams, C.A. (1997): Depositional dynamics of Middle Devonian deposits in the Elk Point Basin: Gilwood Mbr (Watt Mountain Fm), Nipisi Field, northcentral Alberta and Yahatinda Fm (Rocky Mountain Front Ranges); Ph.D. thesis, University of Calgary, 1010 p.
- Zonneveld, J.P., Carrelli, G.G. and Riediger, C. (2004): Sedimentology of the Upper Triassic Charlie Lake, Baldonnel and Pardonet formations from outcrop exposures in the southern Trutch region, northeastern British Columbia; *Bulletin of Canadian Petroleum Geology*, v. 52, p. 343–375.
- Zonneveld, J.P., MacNaughton, R.B. and Utting, J. (2010): Sedimentology and ichnology of the Lower Triassic Montney Formation in the Pedigree-Ring/Border-Kahntah River area, northwestern Alberta and northeastern British Columbia; *Bulletin of Canadian Petroleum Geology*, v. 58, p. 115–140.